

MPPI-Generic: A CUDA Library for Stochastic Optimization

Bogdan Vlahov¹, Jason Gibson¹, Manan Gandhi¹, Evangelos A. Theodorou¹

Abstract—This paper introduces a new C++/CUDA library for GPU-accelerated stochastic optimization called MPPI-Generic. It provides implementations of Model Predictive Path Integral control, Tube-Model Predictive Path Integral Control, and Robust Model Predictive Path Integral Control, and allows for these algorithms to be used across many pre-existing dynamics models and cost functions. Furthermore, researchers can create their own dynamics models or cost functions following our API definitions without needing to change the actual Model Predictive Path Integral Control code. Finally, we compare computational performance to other popular implementations of Model Predictive Path Integral Control over a variety of GPUs to show the real-time capabilities our library can allow for. Library code can be found at: <https://acds-lab.github.io/mppi-generic-website/>

I. INTRODUCTION

As robotics and autonomy continue to grow, the choice of algorithms and methods used to plan and control of complex systems in these fields start to become more selective. These algorithms need to be able to handle the potentially complex dynamics of robotics system and allow representation for complex cost functions. They also need to be responsive to new data as environments and systems change, as in a self-driving scenario. Finally, the planning and control methods used need to be able to run in real-time so that the robot can continue to perform without unnecessary pauses.

The approaches to control optimization can be delineated into two types of methods: gradient-based and sampling-based. Gradient-based methods such as iterative Linear Quadratic Regulator (iLQR) [1], Differential Dynamic Programming (DDP) [2] and Sequential Quadratic Programming (SQP) [3] generally have to rely on some restrictions to the dynamics and cost functions they are applied to such as being continuously differentiable. But in exchange for those restrictions, they can produce controls that minimize the cost function in a computationally-efficient manner. Sampling-based methods, such as Model Predictive Path Integral (MPPI) [4] or Cross-Entropy Method (CEM) [5], can relax these requirements and allow for arbitrary functions but come at the cost of requiring many samples to properly estimate the optimal control. Thus, we can see that while we gain more freedom in representation of functions, we pay for that in computational expense. One way to address this computational expense is to push the computation out of the CPU and onto a GPU. GPUs are designed to be highly parallelizable and for the majority of most sampling-based methods, we want to run the same computations on different inputs. By taking advantage of the

GPU, we can make sampling-based methods usable in real time and also provide enough samples to get optimal solutions.

MPPI utilizes the parallelization offered by GPUs. First introduced in [4], MPPI is a stochastic optimization Model Predictive Control (MPC) algorithm derived using the information theoretic dualities between relative entropy and free energy. Experiments in [4] included off-road navigation using the GT-Autorally vehicle [6] and demonstrated for the first time utilization of GPU for sampling-based MPC on real hardware. Follow-up works included the derivation of MPPI for the case of non-affine dynamics [7], [8] and extensions to multi-layer control architectures that incorporate the benefits of Differential Dynamic Programming to increase robustness to disturbances and model errors. These extensions include the Tube-based MPPI [9], Robust-MPPI (RMPPI) [10] architectures which consists of two layers of control.

Since this first wave of publications on MPPI there has been a plethora of extensions and improvements including Tsallis-MPPI [11], Covariance Control MPPI [12], Constrained Covariance Steering MPPI [13], and Colored MPPI [14], Residual MPPI [15], Biased-MPPI [16], Multi-Modal MPPI [17], Risk-Aware MPPI [18], Spline-Interpolated Model Predictive MPPI [19], Stein Variational Guided MPPI [20], log-MPPI [21], and Smooth MPPI [22]. Besides the obvious use-case of MPC, alternative use-cases of MPPI can be found in the Model-Based Reinforcement Learning (MBRL) literature [23], [24], [25], [26], [27], [28]. In MBRL, MPPI is used to seek data from a simulation environment to learn the underlying value function and corresponding policy. Finally, while the majority of prior work on MPPI has direct applications to planning and control for systems in robotics and autonomy such as quad-rotors [29], [19], terrestrial [4], [14], [21], [30], [31], sea surface [32], [33] and underwater [34] vehicles, manipulators [35] and systems with multi-body dynamics [36], there are notable applications to other domains of science and engineering. These include control of HVAC systems [37], [38], chemical reactors [39], and pulse width modulation rectifiers [40].

Given the far reaches of the MPPI algorithm, it is important to provide a solid and flexible computational framework from which researchers can make use of previous advancements to push their own work forwards. That framework needs to not only provide many built-in options to allow for testing on different platforms but also allow for researchers to develop new ideas on top of. Finally, that library needs to be able to support researchers all the way to hardware deployment with the ability to run in real time even on older hardware platforms.

With this inspiration in mind, we introduce our controls and

¹ Autonomous Control and Decision Systems Lab, Georgia Institute of Technology, Atlanta GA 30313 USA (Corresponding author: Bogdan Vlahov)

planning optimization library, MPPI-Generic. It is written in C++/CUDA and contains multiple dynamics and cost functions to allow for researchers to begin using them in complex robotics scenarios. In addition, it also allows for researchers to create their own dynamics or cost functions that can take advantage of the GPU-accelerated controllers. It provides implementations of MPPI[4], Tube-MPPI[9], and RMPPI [10] as each requires different GPU code to support. If desired, there is an API to allow for implementation of alternative sampling-based controllers. Initial versions of this library have already been used in a variety of hardware and software experiments [14], [32], [10], [41], [42]. To the best of our knowledge, this is the first MPPI library implementation to provide GPU-acceleration with real-time performance, multiple existing dynamics and cost functions, replaceable sampling distributions and controller algorithms, and extensibility options for researchers to create new components.

Our contributions are summarized as follows:

- We provide a NVIDIA GPU-accelerated Library for MPPI.
- We provide a C++/CUDA API that allows for arbitrary dynamics and cost function definitions while maintaining high computational performance. We show simple examples of extending various parts of the library to give researchers an idea of how they could customize this library for their own needs.
- We show computational comparisons with other popular MPPI libraries across a variety of computational hardware.

The rest of the paper is organized as follows: In Section II, we provide the general problem formulation of a stochastic optimization problem and discuss the building blocks of the MPPI-Generic Library. In Section III, we discuss implementation details of our library and performance parameters available to the user to tweak. In Section IV, we show how to use the library through coding examples. In Section V, we show computational comparisons of our library against other implementations of MPPI. Finally, we state our conclusions in Section VI.

II. BACKGROUND

Consider a general nonlinear system with discrete dynamics and cost function of the following form:

$$\mathbf{x}_{t+1} = \mathbf{F}(\mathbf{x}_t, \mathbf{u}_t) \quad (1)$$

$$\mathbf{y}_t = G(\mathbf{x}_t, \mathbf{u}_t) \quad (2)$$

$$\mathbf{J}(Y, U) = \phi(\mathbf{x}_T) + \sum_{t=0}^{T-1} \ell(\mathbf{y}_t, \mathbf{u}_t), \quad (3)$$

where $\mathbf{x} \in \mathbb{R}^{n_x}$ is the state of dimension n_x , $\mathbf{u} \in \mathbb{R}^{n_u}$ is the control of dimension n_u , $\mathbf{y} \in \mathbb{R}^{n_y}$ is the observation of the system in dimension n_y , T is the time horizon, Y is an output trajectory $[\mathbf{y}_1, \mathbf{y}_2, \dots, \mathbf{y}_T]$, U is a control trajectory $[\mathbf{u}_0, \mathbf{u}_1, \dots, \mathbf{u}_{T-1}]$, ϕ is the terminal cost, and ℓ is the running cost.

Looking at the above equations, we can see that there is a minor difference from the typical nonlinear control setup,

shown in Eq. (4), in that we have our cost function using the output, \mathbf{y}_t instead of \mathbf{x}_t .

$$\mathbf{J}(X, U) = \phi(\mathbf{x}_T) + \sum_{t=0}^{T-1} \ell(\mathbf{x}_t, \mathbf{u}_t) \quad (4)$$

For the vast majority of systems, \mathbf{y}_t can just be the true state, i.e. $\mathbf{y}_t = \mathbf{x}_t$ but we have seen that separating the two can be important for computational reasons. It allows reuse of computationally-heavy calculations required for dynamics updates such as wheel position and forces in the cost function. Having this split between \mathbf{x}_t and \mathbf{y}_t is one that allows us to improve the efficiency of the real-time code while not having to do unnecessary computations such as a Jacobian with respect to every wheel position.

It is important to note that the MPPI-Generic dynamics assumes Euler integration by default but can be modified if desired by developing a custom dynamics class.

A. The MPPI Algorithm

MPPI is a stochastic optimal control algorithm that minimizes Eq. (4) through the use of sampling. We start by sampling control trajectories, running each trajectory through the dynamics in Eq. (1) to create a corresponding state trajectory, and then evaluating each state and control trajectory through the cost function. Each trajectory's cost is then run through the exponential transform,

$$S(\mathbf{J}; \lambda) = \exp\left(-\frac{1}{\lambda}\mathbf{J}\right), \quad (5)$$

where λ is the inverse temperature. Finally, a weighted average of the trajectories is conducted to produce the optimal control trajectory. The update law for $\mathcal{U}^*(t)$, the optimal trajectory at time t , ends up looking like

$$\mathcal{U}_t^* = \frac{\sum_{m=1}^M \exp\left(-\frac{1}{\lambda}\mathbf{J}(X^m, V^m)\right) \mathbf{v}_t^m}{\sum_{j=1}^M \exp\left(-\frac{1}{\lambda}\mathbf{J}(X^j, V^j)\right)} \quad (6)$$

$$= \mathbf{u}_t + \frac{\sum_{m=1}^M \exp\left(-\frac{1}{\lambda}\mathbf{J}(X^m, V^m)\right) \epsilon_t^m}{\sum_{j=1}^M \exp\left(-\frac{1}{\lambda}\mathbf{J}(X^j, V^j)\right)}, \quad (7)$$

where V^m is the m -th sampled control trajectory, $\mathbf{v}_t^m = \mathbf{u}_t + \epsilon_t^m$ is the control from the m -th sampled trajectory at time t sampled around the previous optimal control, \mathbf{u}_t , with $\epsilon_t^m \sim \mathcal{N}(0, \sigma^2)$. Sampling in the control space ensures that the trajectories are dynamically feasible and allows us to use non-differentiable dynamics and cost functions. Pseudo code for the algorithm is shown in Algorithm 1.

The original derivation of MPPI was done from a path-integral approach [4]. Future papers then derived MPPI from information theory [8], stochastic search [43], and mirror descent [44] approaches. A Tube-based MPPI controller [9] was also created in order to improve robustness to state disturbances. It made use of a tracking controller to cause the real system to track back to a nominal system that ignored state disturbances resulting in large costs. The nominal system would use the dynamics equation from Eq. (1) to update the initial state for a new iteration of MPPI instead of the real system's state estimate. Both the real and the nominal

Algorithm 1: MPPI

Given: $\mathbf{F}(\cdot, \cdot)$, $G(\cdot, \cdot)$, $\ell(\cdot, \cdot)$, $\phi(\cdot)$ M , I , T , λ , σ : System dynamics, system observation, running cost, terminal cost, num. samples, num. iterations, time horizon, temperature, standard deviations;
Input: \mathbf{x}_0 , \mathbf{U} : initial state, mean control sequence;
Output: \mathcal{U} : optimal control sequence

```
// Begin Cost sampling
1 for  $i \leftarrow 1$  to  $I$  do
2   for  $m \leftarrow 1$  to  $M$  do
3      $J^m \leftarrow 0$ ;
4      $\mathbf{x} \leftarrow \mathbf{x}_0$ ;
5     for  $t \leftarrow 0$  to  $T-1$  do
6        $\mathbf{v}_t \leftarrow \mathbf{u}_t + \epsilon^m(t)$ ,  $\epsilon^m(t) \sim \mathcal{N}(0, \sigma^2)$ ;
7        $\mathbf{x} \leftarrow \mathbf{F}(\mathbf{x}, \mathbf{v}_t)$ ;
8        $\mathbf{y} \leftarrow G(\mathbf{x}, \mathbf{v}_t)$ ;
9        $J^m += \ell(\mathbf{y}, \mathbf{v}_t)$ ;
10     $J^m += \phi(\mathbf{y})$ 
// Compute trajectory weights
11  $\rho \leftarrow \min\{J^1, J^2, \dots, J^M\}$ ;
12  $\eta \leftarrow \sum_{m=1}^M \exp(-\frac{1}{\lambda}(J^m - \rho))$ ;
13 for  $m \leftarrow 1$  to  $M$  do
14    $w_m \leftarrow \frac{1}{\eta} \exp(-\frac{1}{\lambda}(J^m - \rho))$ ;
// Control update
15 for  $t \leftarrow 0$  to  $T-1$  do
16    $\mathcal{U}_t \leftarrow \mathbf{u}_t + \sum_{m=1}^M w_m \epsilon^m(t)$ 
```

trajectories are calculated using MPPI while the tracking controller was iLQR. In this setup, the tracking controller would always be the one sending controls to the system and as MPPI was not aware of the tracking controller, it could end up fighting against the tracking controller. In order to address this, RMPPI was developed in [45], [10], which applied the tracking controller feedback within the samples MPPI used. RMPPI also chose the initial state for the nominal system using a constrained optimization problem that tried to keep the nominal state as close to the real state without causing the resulting trajectory to have a cost larger than a given cost threshold α . Choosing the nominal state in this way ensured there was an upper bound on how quickly the optimal trajectory's cost could grow due to disturbance. Our library contains implementations of these algorithmic improvements to MPPI as different controllers are the best choice in different scenarios.

B. Library Description

This library is made up of 6 major types of classes:

- Dynamics
- Cost Functions
- Controllers
- Sampling Distributions
- Feedback Controllers
- Plants

The Dynamics and Cost Function classes are self-evident and are classes describing the \mathbf{F} , \mathbf{G} , ℓ , and ϕ functions from Eqs. (1) to (3). The Controller class finds the optimal control sequence U that minimizes the cost $\mathbf{J}(Y, U)$ using algorithms such as MPPI. The Sampling Distributions are used by the Controller class to generate the control samples used for determining the optimal control sequence. The Feedback

Controller class determines what feedback controller is used to help push the system back towards the desired trajectory. This is required for the Tube-MPPI and RMPPI implementations but can even be used with the MPPI controller as it provides feedback in between MPC iterations. Unless otherwise specified, the Feedback Controllers in code examples are instantiated but turned off by default. Finally, Plants are a MPC wrapper around a given controller and are where the interface methods in and out of the controller are generally defined. For example, a common-use case of MPPI is on a robotics platform running Robot Operating System (ROS) [46]. The Plant would then be where you would implement your ROS subscribers to information such as state, ROS publishers of the control output, and the necessary methods to convert from ROS messages to MPPI-Generic equivalents. Each class type has their own parameter structures which encapsulate the adjustable parameters of each specific instantiation of the class. For example, the cartpole dynamics parameters include the mass and length of the pendulum whereas a double integrator dynamics system has no additional parameters.

III. PERFORMANCE IMPLEMENTATION

We now will go over some of the performance-specific implementation details we make use of in MPPI-Generic. First, we will give a brief introduction to GPU hardware and terminology followed by general GPU performance tricks. We will then dive into computational optimizations that are specific to the tasks our library is used to solve.

A. GPU Parallelization Overview

The GPU is a highly parallelizable hardware device that performs operations a bit differently from a CPU. The lowest level of computation in CUDA is a *warp*, which consists of 32 threads doing the same operation at every clock step. These warps are grouped together to produce *thread blocks*. The individual warps in the thread block are not guaranteed to be at the same place in the code at any given time and sometimes it can actually be more efficient to allow them to differ. The threads in a thread block all have access a form of a local cache called *shared memory*. Like any memory shared between multiple threads on the CPU, proper mutual exclusion needs to be implemented to avoid race conditions. Threads in a block can be given indices in 3 axes, x , y , and z , which we use to denote different types of parallelization within the library. Thread blocks can themselves be grouped into *grids* and are also organized into x , y , and z axes. This is useful for large parallel operations that cannot fit within a single thread block and also do not need to use shared memory between every thread. The GPU code is compiled into *kernels*, which can then be provided arbitrary grid and block dimensions at runtime.

It is important to briefly understand the hierarchy of memory before discussing how to improve GPU performance. At the highest level, we have *global* memory which is generally measured in GBs and very slow to access data from. Next, we have an L2 cache in the size of MBs which can speed up access to frequently-used global data. Then we have the

L1 cache, shared memory, and CUDA texture caches. The L1 cache and shared memory are actually the same memory on hardware and are generally several kB in size; they are just separated by programmers explicitly using shared memory and the GPU automatically filling the L1 cache. The CUDA texture cache is a fast read-only memory used for CUDA textures which are 2D or 3D representations of data such as a map.

B. General GPU speedups

When looking into writing more performant code, there are some general tricks that we have leveraged throughout our code library. The first is the use of CUDA streams [47]. By default, every call to the GPU blocks the CPU code from moving ahead. CUDA streams allow for the asynchronous scheduling of tasks on the GPU while the CPU performs other work in the meantime. We use CUDA streams throughout in order to schedule memory transfers between the CPU and GPU as well as kernel calls and have different streams for controller optimal control computation and visualization.

The next big tip is minimizing global memory accesses. Global memory reading or writing can be a large bottleneck in computation time and for our library, it can take up more time than the actual computations we want to do on the GPU. The first step recommended is to move everything you can from global memory to shared memory [48]. We also make use of Curiously Recurring Template Patterns (CRTPs) [49] as our choice of polymorphism on the GPU as to avoid the need of constructing and reading from a virtual method table which would need to be stored in global memory. In addition, we utilize vectorized memory [50] accessing where possible. Looking at the GPU instruction set, CUDA provides instructions to read and write in 32, 64, and 128 bit chunks in a single instruction. This means that it is possible to load up to four 32-bit floats in a single instruction. Using these concepts, we greatly reduce the number of calls to global memory and consequently increase the speed at which our computations can run.

C. Library-Specific Performance Optimizations

So far, we have discussed optimizations that can be done for any CUDA program. However, there are further optimizations to be had in choosing how to parallelize specific components of our library. In Fig. 1, we have the general steps taken every time we want to compute a new optimal control sequence in MPPI. These same steps are also taken in Tube-MPPI and RMPPI though they have to be done for both the nominal and real systems.

One major performance consideration is how to parallelize the Dynamics and Cost Function calculations. We have found that, depending on the circumstances and the number of samples used in MPPI, different parallelization techniques make more sense. One way would be to run the Dynamics and Cost Function in a combined kernel on the GPU while another would be to run them in separate kernels. We discuss the description as well as the pros and cons of each parallelization technique below.

1) *Split Kernel Description:* We start by taking the initial state and control samples and run them through the Dynamics kernel. This kernel uses all three axes of thread parallelization for different components. First, the x dimension of the block and the grid are used to indicate which sample we are on as `threadIdx.x + blockDim.x * blockIdx.x`. As every sample should go through the exact same computations, using the x axis allows us to ensure that each *warp* is aligned. Next, the z axis is used to indicate which system is being run; for MPPI, there is only one system but Tube-MPPI and RMPPI use two systems, nominal and real. Finally, the y dimension is used to parallelize within the dynamics function. As dynamics are rarely doing the same derivative computation for every state, this additional parallelization within the dynamics, shown in Lst. 1, can lead to better performance rather than sequentially going through each calculation. In the Dynamics kernel, we

```

1  int tdy = threadIdx.y;
2  switch(tdy) {
3      case S_INDEX(X):
4          xdot[tdy] = u[C_INDEX(VEL)]*cos(x[S_INDEX(YAW)]);
5          break;
6      case S_INDEX(Y):
7          xdot[tdy] = u[C_INDEX(VEL)]*sin(x[S_INDEX(YAW)]);
8          break;
9      case S_INDEX(YAW):
10         xdot[tdy] = u[C_INDEX(YAW_DOT)];
11         break;
12     }

```

Listing 1. GPU code for the Unicycle Dynamics. This code parallelizes using the thread y dimension to do each state derivative calculation in a different thread

then run a `for` loop over time for each sample in which we get the current control sample, runs it through the Dynamic's `step()` method, and save out the resulting output to global memory.

Now, we could have also run the Cost Function inside the previous kernel but we instead separate it out into its own kernel. The reason for that is that while the Dynamics must be sequential over time, the cost function does not need to be. To achieve this, we move the sample index up to the grid level and use the block's x axes for time instead. The Cost kernel gets the control and output corresponding to the current time in its `computeRunningCost()` or `terminalCost()` methods, adds the cost up across time for each sample, and saves out the resulting overall cost for each sample. A problem that might arise with this implementation is that we might become limited in the number of timesteps we could optimize over due there being a limit of 1024 threads in a single thread block. In order to address this, we calculate the max number of iterations over the thread x dimension required to achieve the desired number of timesteps and conduct a `for` loop over that iteration count. So for example, if we had 500 as the desired number of timesteps and block x size of 128, we would do four iterations in our `for` loop to get the total horizon cost. These choices brings the time to do the cost calculation to much closer to that of a single timestep instead of having to wait for sequential iterations of the cost if it was paired with the Dynamics kernel.

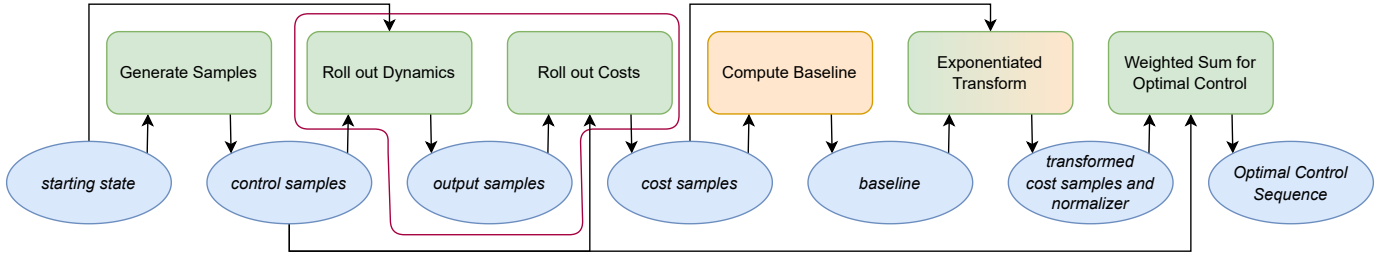


Fig. 1. Diagram of the execution flow of `computeControl()`. The blue ellipses indicate variables, the green rectangles are GPU methods, and the orange rectangles are CPU methods. The selection in purple is a single GPU kernel when using the combined kernel and separated out when using split kernels. Most of the code is run on the GPU but we have found that some operations such as finding the baseline run faster on the CPU.

2) *Combined Kernel Description:* The Combined Kernel runs the Dynamics and Cost Function methods together in a single kernel. This works by getting the initial state and control samples, applying the Dynamics’ `step()` to get the next state and output, and running that output through the Cost Functions’ `computeCost()` to get the cost at that time. This basic interaction is then done in a `for` loop over the time horizon to get the the entire state trajectory as well as the cost of the entire sample. We parallelize this over three axes. First, the x and z dimensions of the block and grid are used to indicate which sample and system we are on as described above in the Split Kernel’s Dynamics section. Finally, the y dimension is used to parallelize within the Dynamics and Cost Functions’ methods.

3) *Choosing between the Split and Combined Kernels:* There are some trade-offs between the two kernel options that can affect the overall computation time. By combining the Dynamics and Cost Function calculations together, we can keep the intermediate outputs in shared memory and don’t need to save them out to global memory. However, we are forced to run the Cost Function sequentially in time. Splitting the Dynamics and Cost Function into separate kernels allows them each to use more shared memory for their internal calculations with the requirement of global memory usage to save out the sampled output trajectories. The Combined Kernel uses less global memory but requires more shared memory usage in a single kernel as it must contain both the Dynamics and Cost Functions’ shared memory requirements. As the number of samples grow, the number of reads and writes of outputs to global memory also grows. This can eventually take more time to do than the savings we get from running the Cost Function in parallel across time, even when using vectorized memory reads and writes.

In order to address these trade-offs, we have implemented both kernel approaches in our library and automatically choose the most appropriate kernel at Controller construction. The automatic kernel selection is done by running both the combined and split kernels multiple times and then choosing the fastest option. As the combined kernel potentially uses more shared memory than the split kernel, we also check to see if the amount of shared memory used is below the GPU’s shared memory hardware limit; if it is not, we default to the split kernel approach. We also allow the user to overwrite the automatic kernel selection through the use of the

`setKernelChoice()` method.

4) *Weight Transform and Update Rule Kernels:* Once the costs of each sample trajectory is calculated, we then bring these costs back to the CPU in order to find the baseline, ρ . The baseline is calculated by finding the minimum cost of all the sample trajectories; it is subtracted out during the exponentiation stage as it has empirically led to better optimization performance. When the number of samples is only in the thousands, we have found that the copy to the CPU to do the baseline search is faster than attempting to do the search on the GPU.

D. Performance Recommendations

The performance capabilities of the MPPI-Generic library is highly dependent on the choices of block sizes for the various kernels, Dynamics, and Cost Functions. There is no one choice to be made so instead, we can provide some general rules of thumbs that we have seen work more often than not.

- Set the thread block x dimension size of both the Dynamics and Cost kernels to be a multiple of 32. This allows all the threads of a warp to be doing the same operation. We have seen in some cases that lowering the thread block x dimension to 16 can provide some improvements but this has not been true for the majority of dynamics and cost functions.
- Set the thread block y dimension of Dynamics and Cost Functions to the state dim and 1 respectively. This depends on whether the Dynamics/Cost Function are utilizing the multi-threading capability available to them but for most of the pre-defined Dynamics, they are using the y axis of the thread block to do dynamics updates. Meanwhile, most Cost Functions are not taking advantage of the multi-threading as they are returning a single value, the cost.
- Keep Dynamics and Cost Function kernels’ thread block sizes low. The limit to the size of a thread block is currently 1024 so it might be tempting to try to fill that. However, there are various synchronization points in these kernels to ensure that data has been loaded before being used. As the thread block size increases, the more time is spent waiting at these synchronization points in the Dynamics and Cost Function kernels.
- When developing your own Dynamics, it can be pertinent to make the output dimensions divisible by 2 or 4.

This can be done by filling the `enum` with filler values. This allows the code to use the more efficient memory loading GPU instructions discussed in Section III-B and reduce the total number of memory calls by a factor of at least 2. One might be tempted to also ensure that the control dimension is divisible by 4. However, the control dimension is also used to generate samples so while there may be improvements to the efficiency of reading memory, it will also take longer to generate samples that are being read.

- Minimize the use of `if` statements in the GPU code when possible. Since GPUs execute a *warp* at a time, having different threads in the warp following different paths of an `if` statement can cause *warp divergence* where every thread ends up executing both code paths by running the `if` statement twice.

IV. API STRUCTURE

We will describe the library API and its usage in three stages. At the beginner level, the desire is to use a provided Dynamics, Cost Function, and Controller to control a system. This requires the least amount of code writing on the part of the user as most of the code is already provided. The library user would only need to write a specific Plant class to properly interface with whatever system they are wanting to control and the executable which sets up and runs the controller itself. The intermediate level is where the user might want to implement a dynamics model or cost function that does not exist in the base library. Finally, at the advanced level, we will show how to implement a custom Feedback Controller, Controller, or Sampling Distribution.

A. Beginner

When using MPPI in a MPC fashion, we need to use a Plant wrapper around our controller. The Plant houses methods to obtain new data such as state, calculate the optimal control sequence at a given rate using the latest information available, and provide the latest control to the external system while providing the necessary tooling to ensure there are no race conditions. As this is the class that provides the interaction between the algorithm and the actual system, it is a component that has to be modified for every use case. For this example, we will implement a plant inheriting from `BasePlant` that houses the external system completely internal to the class. Specifically, we will write our plant to run the dynamics inside `pubControl()` in order to produce a new state. We shall then call `updateState()` at a different fixed rate from the controller re-planning rate to show that the capability of the code base.

In Lst. 3, we can see a simple implementation of a Plant. `SimpleCartpolePlant` instantiates a `CartpoleDynamics` variable upon creation, overwrites the required virtual methods from `BasePlant`, and sets up the dynamics update to occur within `pubControl()`. Looking at the constructor, we pass a shared pointer to a Controller, an integer representing the controller replanning rate, and the minimum timestep we want to adjust the control trajectory by when performing multiple optimal control calculations to the base Plant constructor, and then

create our stand-in system dynamics. `pubControl()` is where we send the control to the system and so in this case, we create necessary extra variables and then pass the current state \mathbf{x}_t and control \mathbf{u}_t as `prev_state` and `u` respectively to the Dynamics' `step()` method to get the next state, \mathbf{x}_{t+1} , in the variable `current_state_`. We also update the current time to show that system has moved forward in time. Looking at this class, a potential issue arises as it is templated on the controller which in turn might not use `CartpoleDynamics` as its Dynamics class. This can be easily remedied by replacing any reference to `CartpoleDynamics` with `CONTROLLER_T::TEMPLATED_DYNAMICS` to make this plant work with the Dynamics used by the instantiated Controller.

Now that we have written our specialized Plant class, we can then go back to the minimal example in Lst. 2 and make some modifications to use the controller a MPC fashion. For this example, we will just run a simple `for` loop that calls the Plant's `runControlIteration()` and `updateState()` methods to simulate a receiving a new state from the system and then calculating a new optimal control sequence from it. The `updateState()` method calls `pubControl()` internally so the system state and the current time will get updated as this runs. For real-time scenarios, there is also the `runControlLoop()` Plant method which can be launched in a separate thread and calls `runControlIteration()` internally at the specified replanning rate.

B. Intermediate

In the previous section, much of the underlying structure of the library was glossed over as it was not necessary to understand. As we get to implementing our own Dynamics or Cost Functions however, there are some basic principles to go over. This library is running code on two different devices, the CPU and the GPU. Some classes, such as Plants and Controllers, don't have methods that need to run on the GPU whereas other classes like the Dynamics and Cost Functions do. The GPU can do many computations in parallel but in order to properly utilize it, that can require different code than what runs on the CPU. As such, when looking at implementing a new Dynamics or Cost Function, there will be some methods that will have to be implemented twice, once for the CPU and once for the GPU.

1) *Custom Dynamics*: Let us first look at Dynamics. The first thing that needs to be implemented for a new Dynamics class is a new parameter structure. We have implemented a dictionary structure in the form of `enum` to define the state, control, and output vectors and these dictionaries are stored in the parameter. For example, in Lst. 4, we show a basic parameter structure implemented for a unicycle model. By implementing these `enum`, we can use these state names later on in the Dynamics and Cost Function to make it clear what state we are referring to. The ending values of `NUM_STATES`, `NUM_CONTROLS`, and `NUM_OUTPUTS` are also used to determine the size of each of the resulting dimensions for creating statically-sized `Eigen::Matrix` data types such as `state_array` and `control_array`.

Next, we need to implement the basic methods needed to be overwritten. These methods are shown in Lst. 5 and

```

1 #include <mppt/controllers/MPPI/mppt_controller.cuh>
2 #include <mppt/cost_functions/cartpole/cartpole_quadratic_cost.cuh>
3 #include <mppt/dynamics/cartpole/cartpole_dynamics.cuh>
4 #include <mppt/feedback_controllers/DDP/ddp.cuh>
5
6 const int NUM_TIMESTEPS = 100;
7 const int NUM_ROLLOUTS = 2048;
8 using DYN_T = CartpoleDynamics;
9 using COST_T = CartpoleQuadraticCost;
10 using FB_T = DDPFeedback<DYN_T, NUM_TIMESTEPS>;
11 using SAMPLING_T = mppt::sampling_distributions::GaussianDistribution<DYN_T::DYN_PARAMS_T>;
12 using CONTROLLER_T = VanillaMPPIController<DYN_T, COST_T, FB_T, NUM_TIMESTEPS, NUM_ROLLOUTS, SAMPLING_T>;
13 using CONTROLLER_PARAMS_T = CONTROLLER_T::TEMPLATED_PARAMS;
14
15 int main(int argc, char** argv) {
16     float dt = 0.02;
17     std::shared_ptr<DYN_T> dynamics = std::make_shared<DYN_T>(); // set up dynamics
18     std::shared_ptr<COST_T> cost = std::make_shared<COST_T>(); // set up cost
19     // set up feedback controller
20     std::shared_ptr<FB_T> fb_controller = std::make_shared<FB_T>(dynamics.get(), dt);
21     // set up sampling distribution
22     SAMPLING_T::SAMPLING_PARAMS_T sampler_params;
23     std::fill(sampler_params.std_dev, sampler_params.std_dev + DYN_T::CONTROL_DIM, 1.0);
24     std::shared_ptr<SAMPLING_T> sampler = std::make_shared<SAMPLING_T>(sampler_params);
25     // set up MPPI Controller
26     CONTROLLER_PARAMS_T controller_params;
27     controller_params.dt_ = dt;
28     controller_params.lambda_ = 1.0;
29     controller_params.dynamics_rollout_dim_ = dim3(64, DYN_T::STATE_DIM, 1);
30     controller_params.cost_rollout_dim_ = dim3(NUM_TIMESTEPS, 1, 1);
31     std::shared_ptr<CONTROLLER_T> controller = std::make_shared<CONTROLLER_T>(
32         dynamics.get(), cost.get(), fb_controller.get(), sampler.get(), controller_params);
33
34     DYN_T::state_array x = dynamics->getZeroState(); // set up initial state
35     controller->computeControl(x, 1); // calculate control
36     auto control_sequence = controller->getControlSeq();
37     std::cout << "Control Sequence:\n" << control_sequence << std::endl;
38     return 0;
39 }

```

Listing 2. Minimal Example to print out optimal control sequence for a cartpole system.

start with `getDynamicsModelName()` which returns the name of the Dynamics model. Next are the CPU and GPU versions of `computeStateDeriv()`. The CPU and GPU versions are differentiated firstly by the `__device__` keyword at the front of the GPU code to designate that method will only live on the GPU. Next, we also only use `Eigen::Matrixf` data-types on the CPU and raw float pointers on the GPU. The `computeStateDeriv()` both would implement the following dynamics,

$$\dot{x} = u_0 * \cos(\psi) \quad (8)$$

$$\dot{y} = u_0 * \sin(\psi) \quad (9)$$

$$\dot{\psi} = u_1, \quad (10)$$

as shown in Lst. 6. You can see here the use of the `enum` we created earlier using the `S_INDEX()` and `C_INDEX()` macros. This allows us to not need to know the order of the states or controls in the underlying data type and more importantly, these same `enum` can also be used in Cost classes to ensure that they are compatible with multiple dynamics as long as the dynamics define the same `enum`.

An important note is that there are separate instances of the class allocated on the CPU and GPU for dynamics and cost functions. In order to update the GPU version you must overwrite `paramsToDevice()` to copy from the CPU side class to the GPU side class. Parameter structures have a default implementation for this, but if helper classes are added their corresponding copy methods will need to be called.

Finally, the last method to be overwritten is `stateFromMap()`. This method is used to translate `std::map` of state names and values into the Dynamics' corresponding state vector. This method ends up being useful for the Plant, especially when different parts of the state can come in at different rates.

The methods listed above are just the beginning of the Dynamics API customization to get started. More advanced customization includes changing the default choice of integration scheme from Euler integration to more accurate integration schemes such as Runge-Kutta or implicit integration if needed, adjusting what is considered the zero state and control for the Dynamics, and adjusting how to linearly interpolate between states.

2) *Custom Cost Function:* If we make a Dynamics class, we also generally will want to make a corresponding Cost. While there is a default quadratic cost implementation that allows for use with any dynamics, we will implement a quick Cost class to show the bare minimum to overwrite. For this example, we will choose to think of our unicycle on a road of some width pointing in the x direction. We want to keep the unicycle on the road so we will penalize the absolute y position linearly up to the road width and then penalize it quadratically if it goes outside the road.

To do this, we will first construct a parameter structure for the cost class. It will inherit from the base `CostParams` class and needs to know the `CONTROL_DIM` and have a variable for the width of the road and coefficient for the cost. From

```

1 #pragma once
2 #include <mppi/core/base_plant.hpp>
3 #include <mppi/dynamics/cartpole/cartpole.cuh>
4
5 template <class CONTROLLER_T> class SimpleCartpolePlant : public class BasePlant<CONTROLLER_T> {
6 public:
7     using control_array = typename CartpoleDynamics::control_array;
8     using state_array = typename CartpoleDynamics::state_array;
9     using output_array = typename CartpoleDynamics::output_array;
10
11     SimpleCartpolePlant(std::shared_ptr<CONTROLLER_T> controller, int hz, int optimization_stride)
12     : BasePlant<CONTROLLER_T>(controller, hz, optimization_stride) {
13         system_dynamics_ = std::make_shared<CartpoleDynamics>();
14     }
15
16     void pubControl(const control_array& u) {
17         state_array state_derivative;
18         output_array dynamics_output;
19         state_array prev_state = current_state_;
20         float t = this->state_time_;
21         float dt = this->controller->getDt();
22         system_dynamics->step(prev_state, current_state_, state_derivative, u, dynamics_output, t, dt);
23         current_time_ += dt;
24     }
25
26     void pubNominalState(const state_array& s) {}
27
28     void pubFreeEnergyStatistics(MPPIFreeEnergyStatistics& fe_stats) {}
29
30     int checkStatus() { return 0; }
31
32     double getCurrentTime() { return current_time_; }
33
34     double getPoseTime() { return this->state_time_; }
35
36     state_array current_state_;
37 protected:
38     std::shared_ptr<CartpoleDynamics> system_dynamics_;
39     double current_time_ = 0.0;
40 }

```

Listing 3. Basic Plant implementation that interacts with a virtual Cartpole dynamics system stored within the Plant.

```

1 struct UnicycleParams : public DynamicsParams {
2     enum class StateIndex : int {
3         X = 0,
4         Y,
5         YAW,
6         NUM_STATES
7     };
8
9     enum class ControlIndex : int {
10        VEL = 0,
11        YAW_DOT,
12        NUM_CONTROLS
13    };
14
15    enum class OutputIndex : int {
16        X = 0,
17        Y,
18        YAW,
19        NUM_OUTPUTS
20    };
21 };

```

Listing 4. Simple parameter structure implementation for a unicycle model

there, we implement a basic Cost class that has to overwrite `computeStateCost()` and `terminalCost()` on both the CPU and GPU sides. It also creates a default constructor and name method `getCostFunctionName()`. This basic implementation can be seen in Lst. 7. Notice that we have created an alias for our dynamics params struct on line 11. This is to allow us to use the `enum` defined there inside our cost function as well.

```

1 class Unicycle : public Dynamics<Unicycle, ↔
2     UnicycleParams> {
3 public:
4     using PARENT_CLASS = Dynamics<Unicycle, ↔
5         UnicycleParams>;
6
7     std::string getDynamicsModelName() const override {
8         return "Unicycle";
9     }
10
11     Unicycle(cudaStream_t stream = nullptr)
12     : PARENT_CLASS(stream) {}
13
14     void computeStateDeriv(
15         const Eigen::Ref<const state_array>& x,
16         const Eigen::Ref<const control_array>& u,
17         Eigen::Ref<state_array> x_dot);
18
19     __device__ inline void computeStateDeriv(
20         float* x, float* u,
21         float* x_dot, float* theta_s);
22
23     state_array stateFromMap(const std::map<std::string↔
24         , float>& map) override;
25 };

```

Listing 5. All the methods that need to be overwritten in a custom Dynamics class

Other things to note are that again, our cost is based on the output rather than the state in `computeStateCost()`. For our simple Unicycle Dynamics, the output is the same as the state.


```

1  xdot[S_INDEX(X)] = u[C_INDEX(VEL)] * cos(x[S_INDEX(↔
   YAW)]);
2  xdot[S_INDEX(Y)] = u[C_INDEX(VEL)] * sin(x[S_INDEX(↔
   YAW)]);
3  xdot[S_INDEX(YAW)] = u[C_INDEX(YAW_DOT)];

```

Listing 6. computeStateDeriv() implementation for a Unicycle dynamics

```

1  struct UnicycleCostParams : public CostParams<↔
   Unicycle::CONTROL_DIM>
2  { float width = 1.0; float coeff = 10.0; };
3
4  class UnicycleCost : public Cost<UnicycleCost, ↔
   UnicycleCostParams, Unicycle::DYN_PARAMS_T>
5  {
6  public:
7      using PARENT_CLASS = Cost<UnicycleCost, ↔
   UnicycleCostParams, Unicycle::DYN_PARAMS_T>;
8      using DYN_P = PARENT_CLASS::TEMPLATED_DYN_PARAMS;
9
10     UnicycleCost(cudaStream_t stream = nullptr);
11
12     std::string getCostFunctionName()
13     { return "Unicycle Cost"; }
14
15     float computeStateCost(
16         const Eigen::Ref<const output_array> y,
17         int t, int* crash_status);
18
19     float terminalCost(
20         const Eigen::Ref<const output_array> y);
21
22     __device__ float computeStateCost(float* y,
23         int t, float* theta_c, int* crash_status);
24
25     __device__ float terminalCost(float* y,
26         float* theta_c);
27 };

```

Listing 7. Basic Cost Function Parameter Structure and Class Implementation for the Unicycle Dynamics

In Lst. 8, the cost function described previously is implemented. We can use `enum` macros such `O_IND_CLASS()` when we are outside of the Dynamics class to still find the appropriate output value. This code can be implemented in both the CPU and GPU `computeStateCost()` methods and we can choose `terminalCost()` to return 0.

```

1  float cost = 0;
2  float y_abs = abs(y[O_IND_CLASS(DYN_P, Y)]);
3  if (y_abs < this->params_.width) {
4      cost = y_abs;
5  } else { // Quadratic cost outside the road width
6      cost = y_abs * y_abs;
7  }
8  return this->params_.coeff * cost;

```

Listing 8. Basic State Cost Implementation for the Unicycle Dynamics

These new Dynamics and Cost could then be easily incorporated into our previous controller examples and that should be enough to get most people started on using this library. There are more options in the Cost and Dynamics classes to improve GPU performance but those are left to Section III.

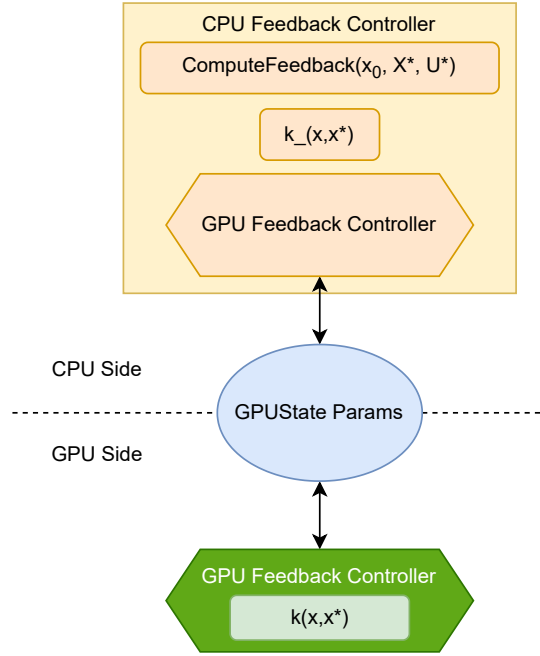


Fig. 2. Feedback Controller API Diagram. We have a GPUState-based parameter structure that contains things like the feedback gains of iLQR. The GPU Feedback Controller class exists both on the GPU (shown in green) and CPU (shown in orange) and contains the GPUState as well as a method $k(x, x^*)$ to calculate the feedback control on the GPU. The CPU Feedback Controller class (shown in yellow) is a wrapper around the GPU Feedback class that has a CPU method to calculate $k(x, x^*)$ as well as a method, `computeFeedback()`, to recompute the feedback gains.

C. Advanced

In this final section, we will show off how to customize Controllers, Feedback Controllers, and Sampling Distributions. Customizing these allows users to create new sampling-based controllers or change the sampling distributions used in specific scenarios.

1) *Feedback Controllers*: One thing we have not yet discussed is the Feedback Controller API. Feedback Controllers are useful even when using MPPI and become necessary for Tube-MPPI and RMPPI. The only Feedback Controller currently implemented is iLQR but we will show how to construct a simple PID controller for each state/control combination.

```

1  template <class DYN_T>
2  class PIDState : public GPUState
3  {
4      using STATE_DIM = DYN_T::STATE_DIM;
5      using CONTROL_DIM = DYN_T::CONTROL_DIM;
6      float p[STATE_DIM * CONTROL_DIM] = {0.0};
7      float i[STATE_DIM * CONTROL_DIM] = {0.0};
8      float d[STATE_DIM * CONTROL_DIM] = {0.0};
9      float dt;
10 };

```

Listing 9. PID Controller Parameter Structure containing the p , i , and d feedback matrices as well as the Δt used for integral and derivative calculations.

Before the example Feedback Controller, we need to go over the code structure for Feedback Controllers as this is very different from the previous examples of Dynamics and

Cost Functions. This is due to the fact that the feedback controller needs to be usable on the GPU but might have different memory requirements on the CPU side. Using iLQR as an example in Fig. 2, calculating the feedback on the GPU would just require the feedback gains to be sent but calculating the feedback gains requires access to the Dynamics and their Jacobians as well as a Cost Function and its Jacobian. To handle this discrepancy in computational workloads, each Feedback Controller is made up of two parts: a GPU feedback class which contains the bare necessities to calculate the feedback, and a CPU wrapper which can do things like recomputing the gains to a new desired trajectory.

Now let us show how to utilize the Feedback Controller API to create a new PID controller. We start by constructing the params structure for the GPU Feedback class, shown in Lst. 9. Note that it is templated off of the Dynamics so that it can create the appropriately-sized arrays for each gain. Since this is a generic PID controller, we will stick to the full feedback matrix representation for each type of gain. Next, we need to implement the GPU Feedback Controller for the PID in Lst. 10. The only method that is required to be overwritten is the $k()$ feedback method but as PIDs require some history to calculate the i and d portions, we will also request extra memory by setting the `SHARED_MEM_REQUEST_BLK_BYTES` variable. This variable allows for extra shared memory per trajectory sample which is necessary for keeping track of history on the GPU.

```

1  template <class DYN_T>
2  class gpuPID : public GPUFeedbackController<gpuPID<←
   DYN_T>, DYN_T, PIDState<DYN_T>> {
3  public:
4  static const int SHARED_MEM_REQUEST_BLK_BYTES = ←
   DYN_T::STATE_DIM * 2;
5
6  __device__ void k(const float* x_act,
7                  const float* x_goal, const int t←
8                  , float* theta, float* u_fb) {
9  int tid = threadIdx.x + blockDim.x * threadIdx.z;
10 float* e_int = theta[(tid * 2 + 0) * DYN_T::←
   STATE_DIM];
11 float* prev_e = theta[(tid * 2 + 1) * DYN_T::←
   STATE_DIM];
12 float e_der[DYN_T::STATE_DIM];
13 float curr_e[DYN_T::STATE_DIM];
14 for (int i = 0; i < DYN_T::STATE_DIM; i++) {
15 curr_e[i] = (x_act[i] - x_goal[i]);
16 e_der[i] = (curr_e[i] - prev_e[i]) / this->state_←
   .dt;
17 e_int[i] += curr_e[i] * this->state_.dt;
18 prev_e[i] = curr_e[i];
19 }
20
21 // start calculating control
22 for (int i = 0; i < DYN_T::CONTROL_DIM; i++) {
23 for (int j = 0; j < DYN_T::STATE_DIM; j++) {
24 int fb_idx = i + j * DYN_T::CONTROL_DIM;
25 u_fb[i] = this->state_.p[fb_idx] * curr_e[j];
26 u_fb[i] += this->state_.i[fb_idx] * e_int[j];
27 u_fb[i] += this->state_.d[fb_idx] * e_der[j];
28 }
29 }
30 }
31 };

```

Listing 10. PID GPU Implementation showing how to implement $k(x, x^*)$ and request shared memory for the integral and derivative of states.

After writing the GPU feedback class, we now just have to write the CPU feedback class, shown in Lst. 11. We only have two methods to overwrite here in `computeFeedback()` and `k_()`. `computeFeedback()` is used to calculate new feedback gains given a new trajectory. For our simple PID class, we will stick to persistent PID gains so this can be left empty. The `k_()` method is just the CPU version of the feedback calculation. For the PID, we can now use member variables to hold the history required to calculate the i and d portions.

2) *Controller*: In order to create a new sampling-based Controller, there are a few methods that must be overwritten. We will walk through how to create a Controller using the CEM [5] as our desired algorithm. Succinctly put, the CEM method samples control trajectories from a Gaussian Distribution, and then uses the best k samples, also known as the elite set, to calculate new parameters for the Gaussian distribution. For this example, we will simplify it to have constant variance and the elite set is used to update the mean of the distribution. The major CEM parameter is the size of the elite set, so we create a new Params struct in Lst. 12 capturing this as a percentage of the total number of samples. From there, the methods that must be overwritten from the base Controller API are `getControllerName()`, `computeControl()`, and `calculateSampledStateTrajectories()`. `getControllerName()` just returns the name of the new controller, i.e. CEM. Next, `computeControl()` is the main method of the Controller class. It takes in the new initial state and calculates the new optimal control sequence from that starting position; an example is shown in Lst. 13. The basic steps are to put the shifted optimal control sequence and initial state onto the GPU, generate the control samples, run the samples through the Dynamics and Cost function, calculate the weights of each sample, use these weights to update the parameters of the sampling distribution, get the new optimal control sequence, and then calculate the corresponding optimal state trajectory. In our example, we add an additional method, `calculateEliteSet()`, to find the elite set and zero out the weights of every other sample specifically for CEM. The final method to overwrite, `calculateSampledStateTrajectories()`, is a method used to generate visualizations based on a subset of sampled trajectories. Users can set a percentage of the sampled trajectories they would like to use for visualization with `setPercentageSampledControlTrajectoriesHelper()` and this method then can be used to generate state trajectories for those samples and put them on the CPU so that they can then be used for visualization purposes. For this simple example, we have no visualization system to plug this data into so we leave this method empty for our CEM implementation.

3) *Sampling Distributions*: The Sampling Distribution class is where the choice of how to sample the control distributions is conducted. Choosing different sampling distributions can have significant changes to the controller performance and is still a large area of research being explored. The current sampling distributions implemented are Gaussian, Colored Noise [14], Normal log-Normal (NLN) noise [21], and Smooth-MPPI [22], but even in those implementations, there are further options and tweaks that we have found to improve performance in the past. Some of these include having a

```

1 public:
2     using PARENT_CLASS = FeedbackController<gpuPID<DYN_T>, PIDParams, NUM_TIMESTEPS>;
3     using control_array = typename PARENT_CLASS::control_array;
4     using state_array = typename PARENT_CLASS::state_array;
5     using state_trajectory = typename PARENT_CLASS::state_trajectory;
6     using control_trajectory = typename PARENT_CLASS::control_trajectory;
7     using INTERNAL_STATE_T = typename PARENT_CLASS::TEMPLATED_FEEDBACK_STATE;
8     using feedback_gain_matrix = typename DYN_T::feedback_matrix;
9
10
11     PIDFeedback(float dt = 0.01, int num_timesteps = NUM_TIMESTEPS, cudaStream_t stream = 0)
12         : PARENT_CLASS(dt, num_timesteps, stream) {
13         this->gpu_controller->getFeedbackStatePointer()->dt = dt;
14     }
15
16     control_array k_(const Eigen::Ref<const state_array>& x_act,
17                    const Eigen::Ref<const state_array>& x_goal,
18                    int t, INTERNAL_STATE_T& fb_state) {
19         Eigen::Map<feedback_gain_matrix> P_gain(&fb_state.p);
20         Eigen::Map<feedback_gain_matrix> I_gain(&fb_state.i);
21         Eigen::Map<feedback_gain_matrix> D_gain(&fb_state.d);
22         state_array curr_e = x_act - x_goal;
23         state_array der_e = (curr_e - prev_e) / this->dt_;
24         e_int_ += (curr_e) * this->dt_;
25         prev_e = curr_e;
26         control_array output = P_gain * curr_e + I_gain * e_int_ + D_gain * der_e;
27         return output;
28     }
29
30     void computeFeedback(const Eigen::Ref<const state_array>& init_state,
31                        const Eigen::Ref<const state_trajectory>& goal_traj,
32                        const Eigen::Ref<const control_trajectory>& control_traj) {}
33
34 protected:
35     state_array e_int_ = state_array::Zero();
36     state_array prev_e_ = state_array::Zero();
37 };

```

Listing 11. PID CPU Implementation. It shows the necessary type aliases and how to compute the feedback control in `k_()`.

percentage of samples sampled from a zero-mean distribution rather than the previous optimal control sequence, using the mean with no noise as a sample, allowing for time-varying standard deviations, and the ability to disable the importance sampling for samples.

The Sampling Distribution API leaves enough flexibility to allow for multi-hypothesis distributions such as Gaussian Mixture Model (GMM) distributions or Stein-Variational distributions [51], [52]. In addition, the `readControlSample()` method used to get the control sample for a particular rollout, time, and system takes in the current output which allows for feedback-based sampling such as done in normalizing flow approaches [53], [54]. The essential methods to focus on if implementing a new Sampling Distribution are `generateSamples()` and `readControlSample()`.

V. BENCHMARKS

In order to see the improvements our library can provide, we decided to compare against three other implementations

```

1 template <int STATE_DIM, int CONTROL_DIM, int MAX_T>
2 struct CEMParams : public ControllerParams<STATE_DIM, ←
3     CONTROL_DIM, MAX_T> {
4     float top_k_percentage = 0.10f;
5 };

```

Listing 12. CEM Controller Parameter Structure containing the percentage of elite samples.

of MPPI publicly available. The first comparison is with the MPPI implementation in AutoRally [55]. This implementation was the starting point of our new library, MPPI-Generic, and so we want to compare to see how well we can perform to our predecessor. The Autorally implementation is written in C++/CUDA, is compatible with ROS, features multiple dynamics models including linear basis functions, simple kinematics, and Neural Network (NN)-based models focused on the Autorally hardware platform. There is only one Cost Function available but it does make use of CUDA textures for doing queries into an obstacle map. Additionally, it has been shown to run in real-time on hardware to great success [6], [4], [8]. However, the Autorally implementation is written mostly for use on the Autorally platform and as such, it has no general Cost Function, Dynamics, or Sampling Distribution APIs to extend. In order to use it for different problems such as flying a quadrotor, the MPPI implementation would need significant modification.

The next implementation we will compare against is ROS2’s MPPI. As of ROS Iron, there is a CPU implementation of MPPI in the ROS navigation stack [56]. This CPU implementation is written in C++ and looks to make heavy use of AVX instructions or vectorized instructions to improve performance. There is a small selection of dynamics models (Differential Drive, Ackermann, and Omni-directional) and cost functions that are focused around wheeled robots navigating through obstacle-laden environments. This implementation will only become more widespread as ROS2 adoption continues to pick

```

1 void computeControl(const Eigen::Ref<const state_array>& state, int optimization_stride = 1) override {
2 // Send the initial condition to the device
3 HANDLE_ERROR(cudaMemcpyAsync(this->initial_state_d_, state.data(), DYN_T::STATE_DIM * sizeof(float),
4                               cudaMemcpyHostToDevice, this->stream_));
5 for (int opt_iter = 0; opt_iter < this->getNumIters(); opt_iter++) {
6   this->copyNominalControlToDevice(false); // Send the optimal control sequence to the device
7   this->sampler->generateSamples(optimization_stride, opt_iter, this->gen_, false); // Generate noise data
8
9   // Calculate state trajectories and costs from sampled control trajectories
10  mppi::kernels::launchSplitRolloutKernel<DYN_T, COST_T, SAMPLING_T>(
11    this->model_->model_d_, this->cost_->cost_d_, this->sampler->sampling_d_, this->getDt(),
12    this->getNumTimesteps(), NUM_SAMPLES, this->getLambda(), this->getAlpha(), this->initial_state_d_,
13    this->output_d_, this->trajectory_costs_d_, this->params_.dynamics_rollout_dim_,
14    this->params_.cost_rollout_dim_, this->stream_, false);
15  // Copy the costs back to the host
16  HANDLE_ERROR(cudaMemcpyAsync(this->trajectory_costs_.data(), this->trajectory_costs_d_,
17                                NUM_SAMPLES * sizeof(float), cudaMemcpyDeviceToHost, this->stream_));
18  HANDLE_ERROR(cudaStreamSynchronize(this->stream_));
19
20  // Setup vector to hold top k weight indices
21  int top_k_to_keep = NUM_SAMPLES * this->params_.top_k_percentage;
22  calculateEliteSet(this->trajectory_costs_, NUM_SAMPLES, top_k_to_keep, top_k_indices_);
23  // keep weights of the elite set
24  float min_elite_value = this->trajectory_costs_[top_k_indices_.back()];
25  std::replace_if(
26    this->trajectory_costs_.data(), this->trajectory_costs_.data() + NUM_SAMPLES,
27    [min_elite_value](float cost) { return cost < min_elite_value; }, 0.0f);
28
29  // Copy weights back to device
30  HANDLE_ERROR(cudaMemcpyAsync(this->trajectory_costs_d_, this->trajectory_costs_.data(),
31                                NUM_SAMPLES * sizeof(float), cudaMemcpyHostToDevice, this->stream_));
32  // Compute the normalizer
33  this->setNormalizer(mppi::common::computeNormalizer(this->trajectory_costs_.data(), NUM_SAMPLES));
34  // Calculate the new mean
35  this->sampler->updateDistributionParamsFromDevice(this->trajectory_costs_d_, this->getNormalizerCost(),
36                                                  0, false);
37  // Transfer the new control back to the host and synchronize stream
38  this->sampler->setHostOptimalControlSequence(this->control_.data(), 0, true);
39  }
40  // Calculate optimal state and output trajectory from the current state and optimal control
41  this->computeOutputTrajectoryHelper(this->output_, this->state_, state, this->control_);
42  }

```

Listing 13. Basic CEM `computeControl()` implementation. This method copies the initial state to the GPU, creates the control samples, calculates the state trajectories and costs of each sample, creates the elite set, updates the mean of the sampling distribution and then copies that mean back as the optimal control sequence.

over the coming years, making it an essential benchmark. Unfortunately, it does have some drawbacks as it is not possible to add new dynamics or cost functions without rewriting the base code itself, has no implementation of Tube-MPPI or RMPPI, and is only available in ROS2 Iron or newer. This means that it might not be usable on existing hardware platforms that are unable to upgrade their systems.

The last implementation of MPPI we will compare against is in TorchRL [57]. TorchRL is an open-source Reinforcement Learning (RL) Python library written by Meta AI, the developers of PyTorch itself. As such, it is widely trusted and available to researchers who are already familiar with PyTorch and Python. The TorchRL implementation works on both CPUs and GPUs and allows for custom dynamics and cost functions through the extension of base Environment class [58]. However, while it does have GPU support, it is limited to the functionality that PyTorch provides meaning that there is no option to use CUDA textures to improve map queries or any direct control of shared memory usage on the GPU. In addition, being written in Python makes it fairly legible and easy to extend but can come at the cost of performance when compared to C++ implementations.

In order to compare our library against these three imple-

mentations, we tried to recreate the same dynamics and cost function for each version of MPPI. As ROS2’s implementation would be the hardest to modify, we chose to use the Differential Drive dynamics model and some of the cost function components that already exist there as the baseline. We ended up using the goal position quadratic cost, goal angle quadratic cost, and the costmap-based obstacle cost components so that we could maintain a fairly simple cost function that allows us to show the capabilities of our library. We implemented these dynamics and cost functions in both CUDA and Python. The CUDA implementations were an extension of our base Dynamics and Cost Function APIs which allowed them to plug into our library easily. We decided to use the same code in the Autorally implementation as well which required some minor rewriting to account for different method names and state dimensions. The Python implementation was an extension of the TorchRL base Environment class, and was compiled using PyTorch’s JIT compiler in order to speed up performance when used in the TorchRL implementation. We used the same parameters for sampling, dynamics, cost function tuning, and MPPI hyperparameters across all implementations, summarized in Table I.

For both Autorally and MPPI-Generic, there are some

further performance enhancing options available such as block size choice. We ended up using the same block sizes for both Autorally and MPPI-Generic across all tests, shown in Table II. As a result, the optimization times shown are not going to be the fastest possible performance that can be achieved on any given GPU but these tests should still serve as a useful benchmark to understand the average performance that can be achieved. We then ran each of the Autorally, MPPI-Generic, and ROS2 implementations 10,000 times to produce optimal trajectories with 128, 256, 512, 1024, 2048, 4096, 6144, 8192, and 16,384 samples; the TorchRL implementation was only run 1000 times due to it being too slow to compute, even when using the GPU. This allowed us to produce more robust measurements of the computation times required as well as understand how well each implementation would scale as more computation was required. While our dynamics and cost functions currently chosen would not need up to 16,394 samples, one might want to implement more complex dynamics or cost functions that could require a large number of samples to find the optimal solution. The comparisons were run across a variety of hardware including a Jetson Nano to see what bottlenecks each implementation might have. The Jetson Nano was unfortunately only able to run the MPPI-Generic and Autorally MPPI implementations as the last supported PyTorch version and the latest TorchRL libraries were incompatible, and the ROS2 implementation was unable to compile. GPUs tested ranged from a NVIDIA GTX 1050 Ti to a NVIDIA RTX 4090. Most tests were performed on an Intel 13900K

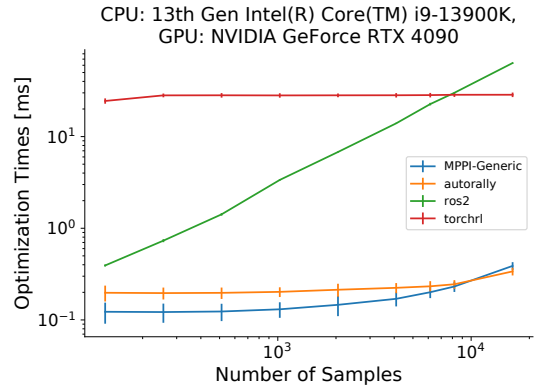


Fig. 3. Optimization times for all MPPI implementations on a hardware system with a RTX 4090 and an Intel 13900K over a variety of number of samples. It can be seen that the ROS2 CPU implementation grows linearly as the number of samples increase while GPU implementations grow more slowly.

which is one of the fastest available CPUs at the time of this writing in order to prevent the CPU being the bottleneck for the mostly GPU-based comparison; however, we did also run some tests on an AMD Ryzen 5 5600x to see the difference in performance on a lower-end CPU. The MPPI optimization times across all the hardware can be seen in Table III and the code used to do these comparisons is available at https://github.com/ACDSL/MPPI_Paper_Example_Code.

A. Results

1) *Differential Drive System*: Going over all of the collected data would take too much room for this paper so we shall instead try to pull out interesting highlights to discuss. Full results can be seen in Table III. First, we can look at the results on the most powerful system tested, using an Intel i9-13900K and an NVIDIA RTX 4090 in Fig. 3. We see that as the number of samples increase, the ROS2 method which is CPU-bound increases in optimization times in a linear fashion. Every other method is on the GPU and we see little reason to use small sample sizes as they have the same computation time till we reach around 1024 samples. We also see that as we hit 16,384 samples, the AutoRally implementation starts to have lower optimization times than MPPI-Generic. We will see this trend continue in Fig. 4.

When looking at older and lower-end NVIDIA hardware such as the GTX 1050 Ti, we still see that our library still performs well compared to other implementations as seen in Fig. 4. Only when the number of samples is at 128 does the ROS2 implementation on an Intel 13900k match the performance of the AutoRally implementation on this older GPU. MPPI-Generic is still more performant at these lower number of samples and eventually we see it scale linearly as we get to thousands of samples. The TorchRL implementation also finally starts to show some GPU bottlenecking as we start to see optimization times increasing as we reach over 6144 samples. We can also see that there is a moment where the MPPI-Generic library optimization time grows to be larger than the AutoRally implementation.

TABLE I
ALGORITHM PARAMETERS

Parameter	Value
dt	0.02 s
wheel radius	1.0 m
wheel length	1.0 m
max velocity	0.5 m/s
min velocity	-0.35 m/s
min rotation	-0.5 rad/s
max rotation	0.5 rad/s
MPPI Parameters	
λ	1.0
control standard deviation	0.2
number of timesteps	100
Cost Parameters	
Dist. to goal coefficient	5
Angular Dist. to goal coeff	5
Obstacle Cost	20
Map width	11 m
Map Height	11 m
Map Resolution	0.1 m/cell

TABLE II
GPU PERFORMANCE CHOICES

Parameter	Value
Dynamics thread block x dim.	64
Dynamics thread block y dim.	4
Cost thread block x dim.	64
Cost thread block y dim.	1

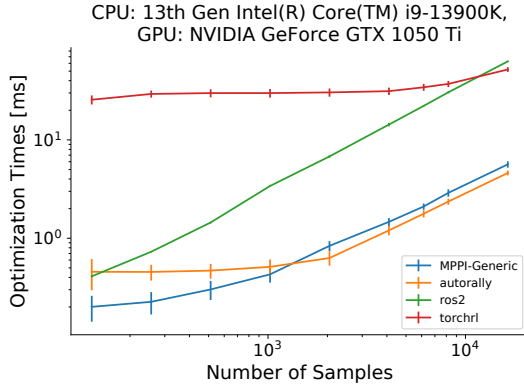


Fig. 4. Optimization times for all MPPI implementations on a hardware system with a GTX 1050 Ti and an Intel 13900K over a variety of number of samples. It can be seen that MPPI-Generic and AutoRally on this older hardware does eventually start to scale linearly with the number of samples but does so at a much lower rate with our library compared to ROS2 or Pytorch.

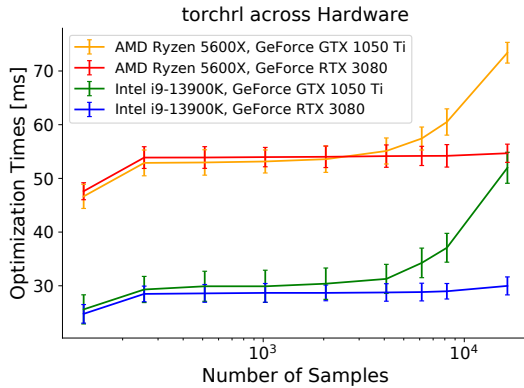


Fig. 5. Optimization times for the TorchRL implementation across different CPUs and GPUs. We see that TorchRL computation times are more dependent on the CPU as the RTX 3080 with an AMD 5600X ends up slower than a GTX 1050 Ti with an Intel 13900k.

That occurs when we switch from using the split kernels (Section III-C1) to the combined kernel (Section III-C2). The AutoRally implementation uses a combined kernel as well but has fewer synchronization points on the GPU due to strictly requiring forward Euler integration for the dynamics. At the small hit to performance in the combined kernel, our library allows for many more features, such as multi-threaded cost functions, use of shared memory in the cost function, and implementation of more computationally-heavy integration methods such as Runge-Kutta or backward Euler integration. And while we see a hit to performance when using the combined kernel compared to AutoRally, we still see that the split kernel is faster for up to 2048 samples.

The TorchRL implementation is notably performing quite poorly in Figs. 3 and 4 with runtimes being around 28ms no matter the number of samples. Looking at TorchRL-specific results in Fig. 5, we can see that the TorchRL implementation seems to be heavily CPU-bound. A low-end GPU (1050 Ti) combined with a high-end CPU (Intel 13900K) can achieve better optimization times than a low-end CPU (AMD 5600X) combined with a high-end GPU (RTX 3080).

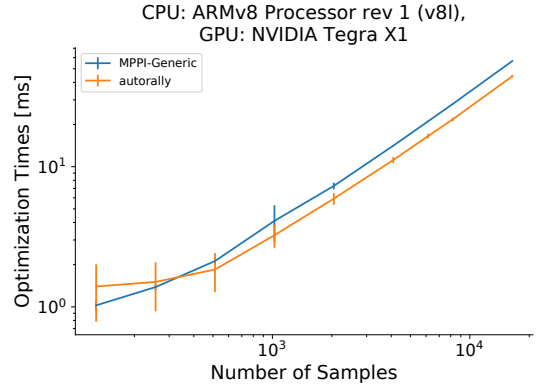


Fig. 6. Optimization times for MPPI implementations on a Jetson Nano over a variety of number of samples. It can be seen that MPPI-Generic and AutoRally on this low-power hardware can still achieve sub 10 ms optimization times for even 2048 samples. The AutoRally implementation quickly surpasses our implementation in optimization times.

We also conducted tests on a Jetson Nano to show that even on relatively low-power and older systems, our library can still be used. As the latest version of CUDA supporting the Jetson Nano is 10.2 and the OS is Ubuntu 18.04, both the pytorch and ROS2 MPPI implementations were not compatible. As such, we only have results comparing our MPPI-Generic implementation to the AutoRally implementation in Fig. 6. Here, we can see that the AutoRally implementation starts having faster compute times around 512 samples. Again, this is due to our library switching to the combined kernel which will be slower. However, our library on a Jetson Nano at 2048 samples has a roughly equivalent computation time to that of 2048 samples of the ROS2 implementation on the Intel 13900K process, showing that our GPU parallelization can allow for real time optimization even on portable systems.

In addition, we can really see the benefits of our library as we increase the computation time of the cost function. At this point, the pytorch and ROS2 implementations have been shown to be slow in comparison to the other implementations and are thus dropped from this cost complexity comparison. We can artificially inflate the computation time of the cost

```

1 float computeStateCost(...) {
2     float cost = 1.0;
3     for (int i = 0; i < NUM_COSINES; i++) {
4         cost = cos(cost);
5     }
6     cost *= 0.0;
7     // Continue to regular cost function
8     ...
9 }

```

Listing 14. Computation time inflation code added to the cost function. We add a configurable amount of calls to `cos()` as this is a computationally heavy function to run.

function with Lst. 14 to judge how well the implementations scale to more complex cost functions. In Fig. 7, we see how increasing the computation time of the cost function scales for both implementations over the same hardware and for the same number of samples.

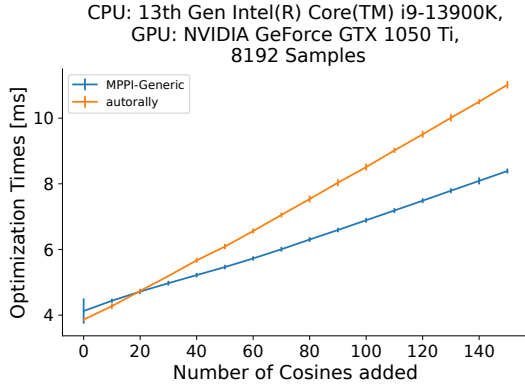


Fig. 7. Optimization Times for MPPI-Generic and AutoRally implementations as the computation time of the cost function increases. Using an Intel 13900K, NVIDIA GTX 1050 Ti, and 8192 samples, we can see that the our library implementation starts to outperform the AutoRally implementation when 20+ sequential cosine operations are added to the cost function.

B. Comparisons to sampling-efficient algorithms

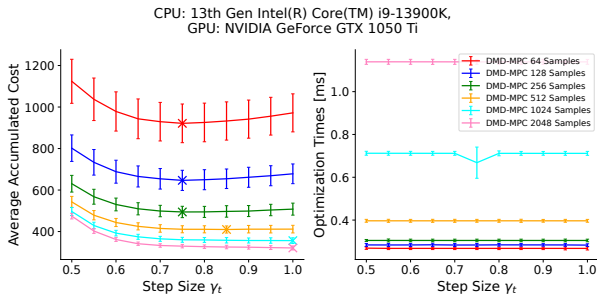


Fig. 8. Average Accumulated Costs (left) and Optimization Times (right) with error bars signifying one standard deviation for a variety of step sizes and number of samples for DMD-MPC. \times indicates the step size that achieves the lowest cost for a given number of samples. This was run on a 2D double integrator dynamics with a cost shown in Eq. (12). This system was run for 1000 timesteps to get the accumulated cost and this was repeated 1000 times to get the standard deviation bars shown. When using a low number of samples, a lower DMD-MPC step size provides the lowest costs. However, as the number of samples increase, the best step size choice becomes $\gamma_t = 1.0$ which is equivalent to the normal MPPI update law. For our library, increasing the number of samples to the point where the step size is no longer useful is still able to be run at over 800 Hz on the NVIDIA GTX 1050 Ti.

While we have shown that our implementation of MPPI can have faster computation times and a lot of flexibility in where it can be applied, there remains a question of what is the balance point between number of samples and real time performance. Ideally, we would like to sample all possible paths to calculate the optimal control trajectory but this is computationally infeasible. While our work has decreased the computation time for sampling which in turn allows more samples in the same computation time, other works have tried to reduce the amount of samples needed to evaluate the optimal control trajectory. In [44], the authors introduce a generalization of MPC algorithms called Dynamic Mirror Descent Model Predictive Control (DMD-MPC) defined by the choice of shaping function, $S(\cdot)$, Sampling Distribution π_θ , and Bregman Divergence $D_\Psi(\cdot, \cdot)$ which determines how close the new optimal control trajectory should remain to the previous. Using the exponential function, Gaussian sampling,

and the Kullback Leibler (KL) Divergence, they derive a slight modification to the MPPI update law in Eq. (7) that introduces a step size parameter $\gamma_t \geq 0$:

$$u_t^{k+1} = (1 - \gamma_t) u_t^k + \gamma_t \frac{\mathbb{E}_{V \sim \pi_\theta} [\mathbf{S}(\mathbf{J}(X, V)) v_t]}{\mathbb{E}_{V \sim \pi_\theta} [\mathbf{S}(\mathbf{J}(X, V))]}, \quad (11)$$

where v_t is the control value at time t from the sampled control sequence V , and \mathbf{J} is the Cost Function from Eq. (3). In their results, they showed that when using a low number of samples, the addition of a step size can help improve performance. However, once the number of samples increases beyond a certain point, the optimal step size ends up being 1.0 which is equivalent to the original MPPI update law. Having this option is useful in cases where you have a low computational budget. What we would like to show is that as long as you have a NVIDIA GPU from the last decade, you can have enough computational budget to just use more samples instead of needing to tune a step size.

Looking at Fig. 8, we ran a 2D double integrator system with state $[x, y, v_x, v_y]$ and control $[a_x, a_y]$ with the cost shown in Eq. (12):

$$J = 1000 \left(\mathbb{I}_{\{(x^2+y^2) \leq 1.875^2\}} + \mathbb{I}_{\{(x^2+y^2) \geq 2.125^2\}} \right) + 2 \left| 2 - \sqrt{v_x^2 + v_y^2} \right| + 2 |4 - (xv_y - yv_x)|. \quad (12)$$

This cost function heavily penalizes the system from leaving a circle of radius 2m with width 0.125m but gives no cost inside the track width, has an L_1 cost on speed to maintain $2m s^{-1}$, and has an L_1 cost on the angular momentum being close to $4m^2/s$. This all combines to encourage the system to move around the circle allowing some small deviation from the center line in a clockwise manner. This system was simulated for 1000 timesteps and the cost was accumulated over that period. This simulation was run 1000 times to ensure consistent cost evaluations. We see that as the number of samples increase, the optimal step size (marked with a \times) increases to 1.0. In addition, the computation time increase for using a number of samples where the step size is irrelevant is minimal (an increase of about 0.04ms).

VI. CONCLUSION

In this paper, we introduce a new sampling-based optimization C++/CUDA library called MPPI-Generic. It contains implementations of MPPI, Tube-MPPI, and RMPPI controllers as well as an API that allows these controllers to be used with multiple dynamics and cost functions. We went through the various ways that researchers could use this library, from using pre-defined dynamics and cost functions to implementing your own sampling-based MPC controller. We also discuss the methods we used to improve the computational performance. We conducted performances comparisons against other widely-available implementations of MPPI over a variety of computer hardware to show the performance benefits our library can provide. Finally, we compared against a sample-efficient form of MPPI to show that with the speed improvements of our library, using more samples is a viable alternative with little hit to computation times. We plan to keep working on the library to add more capabilities and usage improvements such as a Python wrapper in the future.

REFERENCES

- [1] W. Li and E. Todorov, "Iterative Linear Quadratic Regulator Design for Nonlinear Biological Movement Systems," in *Proceedings of the First International Conference on Informatics in Control, Automation and Robotics - Volume 1: ICINCO*, INSTICC. SciTePress, 2004, pp. 222–229. 1
- [2] D. H. Jacobson and D. Q. Mayne, *Differential dynamic programming*, ser. Modern analytic and computational methods in science and mathematics. American Elsevier Pub. Co., 1970. 1
- [3] P. T. Boggs and J. W. Tolle, "Sequential quadratic programming," *Acta numerica*, vol. 4, pp. 1–51, 1995. 1
- [4] G. Williams, P. Drews, B. Goldfain, J. M. Rehg, and E. A. Theodorou, "Aggressive Driving with Model Predictive Path Integral Control," in *2016 IEEE International Conference on Robotics and Automation (ICRA)*. IEEE, 2016, pp. 1433–1440. [Online]. Available: <https://ieeexplore.ieee.org/document/74872771> 1, 2, 11
- [5] R. Rubinstein, "The cross-entropy method for combinatorial and continuous optimization," *Methodology and computing in applied probability*, vol. 1, pp. 127–190, 1999. 1, 10
- [6] B. Goldfain, P. Drews, C. You, M. Barulic, O. Velev, P. Tsiotras, and J. M. Rehg, "AutoRally: An Open Platform for Aggressive Autonomous Driving," *IEEE Control Systems Magazine*, vol. 39, no. 1, pp. 26–55, 2019. 1, 11
- [7] G. Williams, N. Wagener, B. Goldfain, P. Drews, J. M. Rehg, B. Boots, and E. A. Theodorou, "Information theoretic mpc for model-based reinforcement learning," in *2017 IEEE international conference on robotics and automation (ICRA)*. IEEE, 2017, pp. 1714–1721. [Online]. Available: <https://ieeexplore.ieee.org/document/7989202> 1
- [8] G. Williams, P. Drews, B. Goldfain, J. M. Rehg, and E. A. Theodorou, "Information-Theoretic Model Predictive Control: Theory and Applications to Autonomous Driving," *IEEE Transactions on Robotics*, vol. 34, no. 6, pp. 1603–1622, 2018. 1, 2, 11
- [9] G. Williams, B. Goldfain, P. Drews, K. Saigol, J. Rehg, and E. Theodorou, "Robust Sampling Based Model Predictive Control with Sparse Objective Information," in *Robotics: Science and Systems XIV*. Robotics: Science and Systems Foundation, Jun. 2018. [Online]. Available: <http://www.roboticsproceedings.org/rss14/p42.pdf> 1, 2
- [10] M. Gandhi, B. Vlahov, J. Gibson, G. Williams, and E. A. Theodorou, "Robust Model Predictive Path Integral Control: Analysis and Performance Guarantees," *IEEE Robotics and Automation Letters*, vol. 6, no. 2, pp. 1423–1430, Feb. 2021. [Online]. Available: <https://arxiv.org/abs/2102.09027v1> 1, 2, 3
- [11] Z. Wang, O. So, J. Gibson, B. I. Vlahov, M. S. Gandhi, G.-H. Liu, and E. A. Theodorou, "Variational Inference MPC using Tsallis Divergence," *ArXiv*, vol. abs/2104.00241, 2021. [Online]. Available: <https://api.semanticscholar.org/CorpusID:232478502> 1
- [12] J. Yin, Z. Zhang, E. Theodorou, and P. Tsiotras, "Trajectory Distribution Control for Model Predictive Path Integral Control using Covariance Steering," in *2022 International Conference on Robotics and Automation (ICRA)*. IEEE, 2022, pp. 1478–1484. 1
- [13] I. M. Balci, E. Bakolas, B. Vlahov, and E. A. Theodorou, "Constrained Covariance Steering Based Tube-MPPI," in *2022 American Control Conference (ACC)*, 2022, pp. 4197–4202. 1
- [14] B. Vlahov, J. Gibson, D. D. Fan, P. Spieler, A.-a. Agha-mohammadi, and E. A. Theodorou, "Low Frequency Sampling in Model Predictive Path Integral Control," *IEEE Robotics and Automation Letters*, pp. 1–8, 2024. [Online]. Available: <https://ieeexplore.ieee.org/document/10480553> 1, 2, 10
- [15] P. Wang, C. Li, C. Weaver, K. Kawamoto, M. Tomizuka, C. Tang, and W. Zhan, "Residual-MPPI: Online Policy Customization for Continuous Control," *arXiv preprint arXiv:2407.00898*, 2024. 1
- [16] E. Trevisan and J. Alonso-Mora, "Biased-mppi: Informing sampling-based model predictive control by fusing ancillary controllers," *IEEE Robotics and Automation Letters*, vol. 9, no. 6, pp. 5871–5878, 2024, green Open Access added to TU Delft Institutional Repository 'You share, we take care!' - Taverne project <https://www.openaccess.nl/en/you-share-we-take-care> Otherwise as indicated in the copyright section: the publisher is the copyright holder of this work and the author uses the Dutch legislation to make this work public. 1
- [17] Y. Zhang, C. Pezzato, E. Trevisan, C. Salmi, C. H. Corbato, and J. Alonso-Mora, "Multi-Modal MPPI and Active Inference for Reactive Task and Motion Planning," *IEEE Robotics and Automation Letters*, vol. 9, no. 9, pp. 7461–7468, 2024. 1
- [18] J. Yin, Z. Zhang, and P. Tsiotras, "Risk-Aware Model Predictive Path Integral Control Using Conditional Value-at-Risk," in *2023 IEEE International Conference on Robotics and Automation (ICRA)*, 2023, pp. 7937–7943. 1
- [19] T. Miura, N. Akai, K. Honda, and S. Hara, "Spline-Interpolated Model Predictive Path Integral Control with Stein Variational Inference for Reactive Navigation," *ArXiv*, vol. abs/2404.10395, 2024. [Online]. Available: <https://api.semanticscholar.org/CorpusID:269157251> 1
- [20] K. Honda, N. Akai, K. Suzuki, M. Aoki, H. Hosogaya, H. Okuda, and T. Suzuki, "Stein Variational Guided Model Predictive Path Integral Control: Proposal and Experiments with Fast Maneuvering Vehicles," in *IEEE International Conference on Robotics and Automation*. IEEE, 2024 (in print). 1
- [21] I. S. Mohamed, K. Yin, and L. Liu, "Autonomous Navigation of AGVs in Unknown Cluttered Environments: Log-MPPI Control Strategy," *IEEE Robotics and Automation Letters*, vol. 7, no. 4, pp. 10 240–10 247, 2022. 1, 10
- [22] T. Kim, G. Park, K. Kwak, J. Bae, and W. Lee, "Smooth Model Predictive Path Integral Control Without Smoothing," *IEEE Robotics and Automation Letters*, vol. 7, no. 4, pp. 10 406–10 413, 2021. 1, 10
- [23] N. Hansen, X. Wang, and H. Su, "Temporal Difference Learning for Model Predictive Control," in *International Conference on Machine Learning*, 2022. [Online]. Available: <https://api.semanticscholar.org/CorpusID:247318709> 1
- [24] M. Bhardwaj, S. Choudhury, and B. Boots, "Blending MPC & Value Function Approximation for Efficient Reinforcement Learning," in *International Conference on Learning Representations*, 2021. [Online]. Available: https://openreview.net/forum?id=RqCC_00Bg7V 1
- [25] N. Hansen, V. JyothirS, V. Sobal, Y. LeCun, X. Wang, and H. Su, "Hierarchical World Models as Visual Whole-Body Humanoid Controllers," *ArXiv*, vol. abs/2405.18418, 2024. [Online]. Available: <https://api.semanticscholar.org/CorpusID:270068197> 1
- [26] N. Hansen, H. Su, and X. Wang, "TD-MPC2: Scalable, Robust World Models for Continuous Control," *ArXiv*, vol. abs/2310.16828, 2023. [Online]. Available: <https://api.semanticscholar.org/CorpusID:264451720> 1
- [27] Y. Qu, H. Chu, S. Gao, J. Guan, H. Yan, L. Xiao, S. E. Li, and J. Duan, "RL-Driven MPPI: Accelerating Online Control Laws Calculation With Offline Policy," *IEEE Transactions on Intelligent Vehicles*, vol. 9, no. 2, pp. 3605–3616, 2024. 1
- [28] J. Watson and J. Peters, "Inferring Smooth Control: Monte Carlo Posterior Policy Iteration with Gaussian Processes," in *Conference on Robot Learning*. PMLR, 2023, pp. 67–79. [Online]. Available: <https://proceedings.mlr.press/v205/watson23a/watson23a.pdf> 1
- [29] J. Pravitra, K. A. Ackerman, C. Cao, N. Hovakimyan, and E. A. Theodorou, "L1-Adaptive MPPI Architecture for Robust and Agile Control of Multirotors," in *2020 IEEE/RSJ International Conference on Intelligent Robots and Systems (IROS)*. IEEE, 2020, pp. 7661–7666. 1
- [30] T. Han, A. Liu, A. Li, A. Spitzer, G. Shi, and B. Boots, "Model Predictive Control for Aggressive Driving over Uneven Terrain," *arXiv preprint arXiv:2311.12284*, 2023. 1
- [31] H. Homburger, S. Wirtensohn, and J. Reuter, "Efficient Nonlinear Model Predictive Path Integral Control for Stochastic Systems considering Input Constraints," in *2023 European Control Conference (ECC)*, 2023, pp. 1–6. 1
- [32] A. M. Patel, M. J. Bays, E. N. Evans, J. R. Eastridge, and E. A. Theodorou, "Model-Predictive Path-Integral Control of an Unmanned Surface Vessel with Wave Disturbance," in *OCEANS 2023 - MTS/IEEE U.S. Gulf Coast*, Sep. 2023, pp. 1–7. [Online]. Available: <https://ieeexplore.ieee.org/document/10336978> 1, 2
- [33] E. Liu, D. Wang, Z. Peng, L. Liu, and N. Gu, "Data-driven Path Following of Unmanned Surface Vehicles based on Model-Based Reinforcement Learning and Model Predictive Path Integral Control," in *2022 37th Youth Academic Annual Conference of Chinese Association of Automation (YAC)*, 2022, pp. 1045–1049. 1
- [34] P. Nicolay, Y. Petillot, M. Marfeychuk, S. Wang, and I. Carlucho, "Enhancing AUV Autonomy with Model Predictive Path Integral Control," in *OCEANS 2023 - MTS/IEEE U.S. Gulf Coast*, 2023, pp. 1–10. 1
- [35] W. Wu, Z. Chen, and H. Zhao, "Model Predictive Path Integral Control based on Model Sampling," in *2019 2nd International Conference of Intelligent Robotic and Control Engineering (IRCE)*, 2019, pp. 46–50. 1
- [36] C. Pan, Z. Peng, Y. Li, B. Han, and D. Wang, "Flocking of Under-Actuated Unmanned Surface Vehicles via Deep Reinforcement Learning and Model Predictive Path Integral Control," *IEEE Transactions on Instrumentation and Measurement*, vol. 73, pp. 1–11, 2024. 1

- [37] Z. An, X. Ding, A. Rathee, and W. Du, “Clue: Safe model-based rl hvac control using epistemic uncertainty estimation,” in *Proceedings of the 10th ACM International Conference on Systems for Energy-Efficient Buildings, Cities, and Transportation*, ser. BuildSys ’23. New York, NY, USA: Association for Computing Machinery, 2023, p. 149–158. [Online]. Available: <https://doi.org/10.1145/3600100.3623742> 1
- [38] X. Ding, A. Cerpa, and W. Du, “Multi-Zone HVAC Control With Model-Based Deep Reinforcement Learning,” *IEEE Transactions on Automation Science and Engineering*, pp. 1–19, 2024. 1
- [39] L. Ai, Y. Chen, Y. Xu, X. Chen, and K. L. Teo, “Model Predictive Path Integral Control of a Temperature Profile in Tubular Chemical Reactor with Recycle,” in *2024 3rd Conference on Fully Actuated System Theory and Applications (FASTA)*, 2024, pp. 1271–1276. 1
- [40] J. Duan, D. Wang, Z. Wang, Z. Peng, L. Liu, and J. Chen, “Finite Set Model Predictive Path Integral Control of Three-Level PWM Rectifier Based on Neural Network Observer,” in *2023 8th Asia Conference on Power and Electrical Engineering (ACPEE)*, 2023, pp. 1942–1948. 1
- [41] M. Gandhi, H. Almubarak, Y. Aoyama, and E. Theodorou, “Safety in Augmented Importance Sampling: Performance Bounds for Robust MPPI,” Apr. 2022. [Online]. Available: <http://arxiv.org/abs/2204.05963> 2
- [42] J. Gibson, B. Vlahov, D. Fan, P. Spieler, D. Pastor, A.-a. Aghamohammadi, and E. A. Theodorou, “A Multi-step Dynamics Modeling Framework For Autonomous Driving In Multiple Environments,” in *2023 IEEE International Conference on Robotics and Automation (ICRA)*. IEEE, May 2023, pp. 7959–7965. 2
- [43] Z. Wang, O. So, K. Lee, and E. A. Theodorou, “Adaptive Risk Sensitive Model Predictive Control with Stochastic Search,” in *Proceedings of the 3rd Conference on Learning for Dynamics and Control*. PMLR, 2021, pp. 510–522. 2
- [44] N. Wagnen, C.-A. Cheng, J. Sacks, and B. Boots, “An Online Learning Approach to Model Predictive Control,” in *Proceedings of Robotics: Science and Systems*, Freiburg im Breisgau, Germany, Jun. 2019. [Online]. Available: <http://arxiv.org/abs/1902.08967> 2, 15
- [45] G. R. Williams, “Model Predictive Path Integral Control: Theoretical Foundations and Applications to Autonomous Driving,” 2019. 3
- [46] S. Macenski, T. Foote, B. Gerkey, C. Lalancette, and W. Woodall, “Robot Operating System 2: Design, Architecture, and Uses in the Wild,” *Science Robotics*, vol. 7, no. 66, p. eabm6074, May 2022. [Online]. Available: <https://www.science.org/doi/10.1126/scirobotics.abm6074> 3
- [47] M. Harris, “How to Overlap Data Transfers in CUDA C/C++,” Dec. 2012. [Online]. Available: <https://developer.nvidia.com/blog/how-overlap-data-transfers-cuda-cc/> 4
- [48] —, “Using Shared Memory in CUDA C/C++,” Jan. 2013. [Online]. Available: <https://developer.nvidia.com/blog/using-shared-memory-cuda-cc/> 4
- [49] J. O. Coplien, “Curiously Recurring Template Patterns,” *C++ Report*, vol. 7, no. 2, pp. 24–27, 1995. 4
- [50] J. Luitjens, “CUDA Pro Tip: Increase Performance with Vectorized Memory Access,” Dec. 2013. [Online]. Available: <https://developer.nvidia.com/blog/cuda-pro-tip-increase-performance-with-vectorized-memory-access/> 4
- [51] Z. Wang, O. So, J. Gibson, B. Vlahov, M. S. Gandhi, G.-H. Liu, and E. A. Theodorou, “Variational Inference MPC using Tsallis Divergence,” in *Robotics: Science and Systems XVII*. Robotics: Science and Systems Foundation, Apr. 2021. 11
- [52] A. Lambert, F. Ramos, B. Boots, D. Fox, and A. Fishman, “Stein Variational Model Predictive Control,” in *Proceedings of the 2020 Conference on Robot Learning*. PMLR, 2021, pp. 1278–1297. 11
- [53] T. Power and D. Berenson, “Variational Inference MPC using Normalizing Flows and Out-of-Distribution Projection,” in *Robotics: Science and Systems XVIII*. Robotics: Science and Systems Foundation, Jun. 2022. 11
- [54] J. Sacks and B. Boots, “Learning Sampling Distributions for Model Predictive Control,” in *Proceedings of The 6th Conference on Robot Learning*. PMLR, Mar. 2023, pp. 1733–1742. 11
- [55] B. Goldfain, P. Drews, G. Williams, and J. Gibson, “AutoRally,” Georgia Tech AutoRally Organization. [Online]. Available: <https://github.com/AutoRally/autorally> 11
- [56] A. Budyakov and S. Macenski, “ROS2 Model Predictive Path Integral Controller,” Open Robotics. [Online]. Available: https://github.com/ros-planning/navigation2/tree/iron/nav2_mppi_controller 11
- [57] A. Bou, M. Bettini, S. Dittert, V. Kumar, S. Sodhani, X. Yang, G. D. Fabritiis, and V. Moens, “TorchRL: A data-driven decision-making library for PyTorch,” in *The Twelfth International Conference on Learning Representations*, Jan. 2024. [Online]. Available: <https://openreview.net/forum?id=QxItoEAVMb> 12
- [58] torchrl contributors, “mppi.py · pytorch/rl,” Meta, 2023. [Online]. Available: <https://github.com/pytorch/rl/blob/main/torchrl/modules/planners/mppi.py> 12

TABLE III
MPPI METHOD OPTIMIZATION TIMES AT VARIOUS NUMBER OF SAMPLES ON VARIOUS HARDWARE

CPU	GPU	Samples	Method	Avg. Time [ms]	CPU	GPU	Samples	Method	Avg. Time [ms]
Intel 13900K	1060 6GB	128	MPPI-Generic	0.180 ± 0.035	Intel 13900K	1080 Ti	128	MPPI-Generic	0.179 ± 0.029
Intel 13900K	1060 6GB	128	autorally	0.436 ± 0.054	Intel 13900K	1080 Ti	128	autorally	0.44 ± 0.12
Intel 13900K	1060 6GB	128	torchrl	24.6 ± 1.6	Intel 13900K	1080 Ti	128	torchrl	24.6 ± 1.8
Intel 13900K	1060 6GB	256	MPPI-Generic	0.191 ± 0.031	Intel 13900K	1080 Ti	256	MPPI-Generic	0.184 ± 0.029
Intel 13900K	1060 6GB	256	autorally	0.432 ± 0.037	Intel 13900K	1080 Ti	256	autorally	0.439 ± 0.036
Intel 13900K	1060 6GB	256	torchrl	28.4 ± 1.4	Intel 13900K	1080 Ti	256	torchrl	28.4 ± 1.4
Intel 13900K	1060 6GB	512	MPPI-Generic	0.226 ± 0.031	Intel 13900K	1080 Ti	512	MPPI-Generic	0.201 ± 0.031
Intel 13900K	1060 6GB	512	autorally	0.434 ± 0.039	Intel 13900K	1080 Ti	512	autorally	0.442 ± 0.038
Intel 13900K	1060 6GB	512	torchrl	28.6 ± 1.6	Intel 13900K	1080 Ti	512	torchrl	28.4 ± 1.6
Intel 13900K	1060 6GB	1024	MPPI-Generic	0.310 ± 0.035	Intel 13900K	1080 Ti	1024	MPPI-Generic	0.220 ± 0.030
Intel 13900K	1060 6GB	1024	autorally	0.467 ± 0.043	Intel 13900K	1080 Ti	1024	autorally	0.448 ± 0.038
Intel 13900K	1060 6GB	1024	torchrl	28.4 ± 1.7	Intel 13900K	1080 Ti	1024	torchrl	28.5 ± 1.6
Intel 13900K	1060 6GB	2048	MPPI-Generic	0.479 ± 0.039	Intel 13900K	1080 Ti	2048	MPPI-Generic	0.298 ± 0.033
Intel 13900K	1060 6GB	2048	autorally	0.545 ± 0.067	Intel 13900K	1080 Ti	2048	autorally	0.482 ± 0.041
Intel 13900K	1060 6GB	2048	torchrl	28.6 ± 1.5	Intel 13900K	1080 Ti	2048	torchrl	28.7 ± 1.4
Intel 13900K	1060 6GB	4096	MPPI-Generic	0.890 ± 0.054	Intel 13900K	1080 Ti	4096	MPPI-Generic	0.432 ± 0.040
Intel 13900K	1060 6GB	4096	autorally	0.986 ± 0.078	Intel 13900K	1080 Ti	4096	autorally	0.549 ± 0.042
Intel 13900K	1060 6GB	4096	torchrl	29.3 ± 1.7	Intel 13900K	1080 Ti	4096	torchrl	28.9 ± 1.7
Intel 13900K	1060 6GB	6144	autorally	1.143 ± 0.077	Intel 13900K	1080 Ti	6144	autorally	0.619 ± 0.041
Intel 13900K	1060 6GB	6144	MPPI-Generic	1.311 ± 0.063	Intel 13900K	1080 Ti	6144	MPPI-Generic	0.702 ± 0.046
Intel 13900K	1060 6GB	6144	torchrl	30.9 ± 1.7	Intel 13900K	1080 Ti	6144	torchrl	29.2 ± 1.7
Intel 13900K	1060 6GB	8192	autorally	1.599 ± 0.071	Intel 13900K	1080 Ti	8192	autorally	0.695 ± 0.047
Intel 13900K	1060 6GB	8192	MPPI-Generic	1.755 ± 0.070	Intel 13900K	1080 Ti	8192	MPPI-Generic	1.109 ± 0.058
Intel 13900K	1060 6GB	8192	torchrl	31.7 ± 1.4	Intel 13900K	1080 Ti	8192	torchrl	29.7 ± 1.5
Intel 13900K	1060 6GB	16384	autorally	3.05 ± 0.64	Intel 13900K	1080 Ti	16384	autorally	1.334 ± 0.061
Intel 13900K	1060 6GB	16384	MPPI-Generic	3.337 ± 0.099	Intel 13900K	1080 Ti	16384	MPPI-Generic	2.188 ± 0.078
Intel 13900K	1060 6GB	16384	torchrl	41.3 ± 1.6	Intel 13900K	1080 Ti	16384	torchrl	33.8 ± 1.6
Intel 13900K	2080	128	MPPI-Generic	0.166 ± 0.023	Intel 13900K	4090	128	MPPI-Generic	0.123 ± 0.032
Intel 13900K	2080	128	autorally	0.29 ± 0.14	Intel 13900K	4090	128	autorally	0.198 ± 0.039
Intel 13900K	2080	128	torchrl	24.8 ± 1.6	Intel 13900K	4090	128	torchrl	24.5 ± 1.6
Intel 13900K	2080	256	MPPI-Generic	0.171 ± 0.024	Intel 13900K	4090	256	MPPI-Generic	0.122 ± 0.029
Intel 13900K	2080	256	autorally	0.292 ± 0.028	Intel 13900K	4090	256	autorally	0.196 ± 0.029
Intel 13900K	2080	256	torchrl	28.6 ± 1.3	Intel 13900K	4090	256	torchrl	28.2 ± 1.3
Intel 13900K	2080	512	MPPI-Generic	0.180 ± 0.028	Intel 13900K	4090	512	MPPI-Generic	0.124 ± 0.026
Intel 13900K	2080	512	autorally	0.299 ± 0.032	Intel 13900K	4090	512	autorally	0.197 ± 0.028
Intel 13900K	2080	512	torchrl	28.7 ± 1.5	Intel 13900K	4090	512	torchrl	28.2 ± 1.6
Intel 13900K	2080	1024	MPPI-Generic	0.204 ± 0.028	Intel 13900K	4090	1024	MPPI-Generic	0.131 ± 0.025
Intel 13900K	2080	1024	autorally	0.302 ± 0.028	Intel 13900K	4090	1024	autorally	0.202 ± 0.025
Intel 13900K	2080	1024	torchrl	28.8 ± 1.5	Intel 13900K	4090	1024	torchrl	28.1 ± 1.6
Intel 13900K	2080	2048	MPPI-Generic	0.261 ± 0.026	Intel 13900K	4090	2048	MPPI-Generic	0.146 ± 0.036
Intel 13900K	2080	2048	autorally	0.323 ± 0.033	Intel 13900K	4090	2048	autorally	0.214 ± 0.035
Intel 13900K	2080	2048	torchrl	28.8 ± 1.3	Intel 13900K	4090	2048	torchrl	28.2 ± 1.3
Intel 13900K	2080	4096	MPPI-Generic	0.398 ± 0.034	Intel 13900K	4090	4096	MPPI-Generic	0.170 ± 0.030
Intel 13900K	2080	4096	autorally	0.403 ± 0.035	Intel 13900K	4090	4096	autorally	0.224 ± 0.028
Intel 13900K	2080	4096	torchrl	29.1 ± 1.6	Intel 13900K	4090	4096	torchrl	28.2 ± 1.6
Intel 13900K	2080	6144	autorally	0.518 ± 0.040	Intel 13900K	4090	6144	MPPI-Generic	0.201 ± 0.028
Intel 13900K	2080	6144	MPPI-Generic	0.576 ± 0.042	Intel 13900K	4090	6144	autorally	0.233 ± 0.032
Intel 13900K	2080	6144	torchrl	29.1 ± 1.6	Intel 13900K	4090	6144	torchrl	28.4 ± 1.6
Intel 13900K	2080	8192	autorally	0.580 ± 0.044	Intel 13900K	4090	8192	MPPI-Generic	0.232 ± 0.030
Intel 13900K	2080	8192	MPPI-Generic	0.705 ± 0.043	Intel 13900K	4090	8192	autorally	0.245 ± 0.027
Intel 13900K	2080	8192	torchrl	29.4 ± 1.3	Intel 13900K	4090	8192	torchrl	28.6 ± 1.5
Intel 13900K	2080	16384	autorally	1.192 ± 0.059	Intel 13900K	4090	16384	autorally	0.338 ± 0.033
Intel 13900K	2080	16384	MPPI-Generic	1.418 ± 0.061	Intel 13900K	4090	16384	MPPI-Generic	0.389 ± 0.038
Intel 13900K	2080	16384	torchrl	32.4 ± 1.5	Intel 13900K	4090	16384	torchrl	28.6 ± 1.6

CPU	GPU	Samples	Method	Avg. Time [ms]	CPU	GPU	Samples	Method	Avg. Time [ms]
AMD 5600X	3080	128	MPPI-Generic	0.1554 ± 0.0156	Intel 13900K	3080	128	MPPI-Generic	0.1475 ± 0.0316
AMD 5600X	3080	128	autorally	0.2701 ± 0.0169	Intel 13900K	3080	128	autorally	0.245 ± 0.118
AMD 5600X		128	ros2	0.6153 ± 0.0319	Intel 13900K		128	ros2	0.3899 ± 0.0162
AMD 5600X	3080	128	torchrl	47.61 ± 1.58	Intel 13900K	3080	128	torchrl	24.77 ± 1.73
AMD 5600X	3080	256	MPPI-Generic	0.1536 ± 0.0336	Intel 13900K	3080	256	MPPI-Generic	0.1526 ± 0.0271
AMD 5600X	3080	256	autorally	0.2743 ± 0.0152	Intel 13900K	3080	256	autorally	0.2428 ± 0.0294
AMD 5600X		256	ros2	1.0804 ± 0.0427	Intel 13900K		256	ros2	0.7290 ± 0.0101
AMD 5600X	3080	256	torchrl	53.88 ± 2.02	Intel 13900K	3080	256	torchrl	28.49 ± 1.45
AMD 5600X	3080	512	MPPI-Generic	0.1528 ± 0.0115	Intel 13900K	3080	512	MPPI-Generic	0.1536 ± 0.0345
AMD 5600X	3080	512	autorally	0.2696 ± 0.0123	Intel 13900K	3080	512	autorally	0.2466 ± 0.0369
AMD 5600X		512	ros2	2.1011 ± 0.0962	Intel 13900K		512	ros2	1.4186 ± 0.0445
AMD 5600X	3080	512	torchrl	53.89 ± 2.02	Intel 13900K	3080	512	torchrl	28.58 ± 1.65
AMD 5600X	3080	1024	MPPI-Generic	0.1704 ± 0.0155	Intel 13900K	3080	1024	MPPI-Generic	0.1634 ± 0.0271
AMD 5600X	3080	1024	autorally	0.2757 ± 0.0148	Intel 13900K	3080	1024	autorally	0.2599 ± 0.0357
AMD 5600X		1024	ros2	4.752 ± 0.240	Intel 13900K		1024	ros2	3.3559 ± 0.0350
AMD 5600X	3080	1024	torchrl	53.97 ± 1.80	Intel 13900K	3080	1024	torchrl	28.68 ± 1.75
AMD 5600X	3080	2048	MPPI-Generic	0.1973 ± 0.0138	Intel 13900K	3080	2048	MPPI-Generic	0.1918 ± 0.0331
AMD 5600X	3080	2048	autorally	0.2850 ± 0.0143	Intel 13900K	3080	2048	autorally	0.2621 ± 0.0390
AMD 5600X		2048	ros2	9.500 ± 0.380	Intel 13900K		2048	ros2	6.7212 ± 0.0651
AMD 5600X	3080	2048	torchrl	54.02 ± 2.00	Intel 13900K	3080	2048	torchrl	28.68 ± 1.46
AMD 5600X	3080	4096	MPPI-Generic	0.2562 ± 0.0377	Intel 13900K	3080	4096	MPPI-Generic	0.2489 ± 0.0388
AMD 5600X	3080	4096	autorally	0.2896 ± 0.0143	Intel 13900K	3080	4096	autorally	0.2760 ± 0.0426
AMD 5600X		4096	ros2	19.583 ± 0.789	Intel 13900K		4096	ros2	13.917 ± 0.152
AMD 5600X	3080	4096	torchrl	54.15 ± 2.08	Intel 13900K	3080	4096	torchrl	28.76 ± 1.63
AMD 5600X	3080	6144	MPPI-Generic	0.3145 ± 0.0194	Intel 13900K	3080	6144	MPPI-Generic	0.3064 ± 0.0391
AMD 5600X	3080	6144	autorally	0.3362 ± 0.0143	Intel 13900K	3080	6144	autorally	0.3243 ± 0.0430
AMD 5600X		6144	ros2	29.872 ± 0.864	Intel 13900K		6144	ros2	21.739 ± 0.189
AMD 5600X	3080	6144	torchrl	54.18 ± 1.79	Intel 13900K	3080	6144	torchrl	28.83 ± 1.65
AMD 5600X	3080	8192	autorally	0.3664 ± 0.0167	Intel 13900K	3080	8192	MPPI-Generic	0.3590 ± 0.0371
AMD 5600X	3080	8192	MPPI-Generic	0.3693 ± 0.0210	Intel 13900K	3080	8192	autorally	0.3605 ± 0.0449
AMD 5600X		8192	ros2	40.64 ± 1.06	Intel 13900K		8192	torchrl	28.98 ± 1.44
AMD 5600X	3080	8192	torchrl	54.20 ± 2.09	Intel 13900K	3080	8192	ros2	29.917 ± 0.239
AMD 5600X	3080	16384	autorally	0.5121 ± 0.0183	Intel 13900K	3080	16384	autorally	0.4991 ± 0.0497
AMD 5600X	3080	16384	MPPI-Generic	0.5790 ± 0.0241	Intel 13900K	3080	16384	MPPI-Generic	0.6271 ± 0.0475
AMD 5600X		16384	torchrl	54.68 ± 1.70	Intel 13900K		16384	torchrl	29.98 ± 1.67
AMD 5600X	3080	16384	ros2	84.26 ± 1.65	Intel 13900K	3080	16384	ros2	62.264 ± 0.990
ARMv8 (v8l)	Tegra X1	128	MPPI-Generic	1.0244 ± 0.0914	ARMv8 (v8l)	Tegra X1	128	autorally	1.397 ± 0.613
ARMv8 (v8l)	Tegra X1	256	MPPI-Generic	1.3839 ± 0.0614	ARMv8 (v8l)	Tegra X1	256	autorally	1.506 ± 0.576
ARMv8 (v8l)	Tegra X1	512	autorally	1.847 ± 0.575	ARMv8 (v8l)	Tegra X1	512	MPPI-Generic	2.123 ± 0.120
ARMv8 (v8l)	Tegra X1	1024	autorally	3.245 ± 0.608	ARMv8 (v8l)	Tegra X1	1024	MPPI-Generic	4.11 ± 1.20
ARMv8 (v8l)	Tegra X1	2048	autorally	5.921 ± 0.578	ARMv8 (v8l)	Tegra X1	2048	MPPI-Generic	7.297 ± 0.399
ARMv8 (v8l)	Tegra X1	4096	autorally	11.159 ± 0.581	ARMv8 (v8l)	Tegra X1	4096	MPPI-Generic	14.124 ± 0.133
ARMv8 (v8l)	Tegra X1	6144	autorally	16.546 ± 0.605	ARMv8 (v8l)	Tegra X1	6144	MPPI-Generic	21.075 ± 0.229
ARMv8 (v8l)	Tegra X1	8192	autorally	21.767 ± 0.629	ARMv8 (v8l)	Tegra X1	8192	MPPI-Generic	28.022 ± 0.261
ARMv8 (v8l)	Tegra X1	16384	autorally	44.158 ± 0.947	ARMv8 (v8l)	Tegra X1	16384	MPPI-Generic	56.650 ± 0.351

CPU	GPU	Samples	Method	Avg. Time [ms]	CPU	GPU	Samples	Method	Avg. Time [ms]
AMD 5600X	1050 Ti	MPPI-Generic	128	0.2149±0.0478	Intel 13900K	1050 Ti	MPPI-Generic	128	0.2008 ± 0.0591
AMD 5600X	1050 Ti	autorally	128	0.4646±0.0337	Intel 13900K	1050 Ti	autorally	128	0.456 ± 0.160
AMD 5600X	1050 Ti	torchrl	128	46.65±2.25	Intel 13900K	1050 Ti	torchrl	128	25.60 ± 2.71
AMD 5600X	1050 Ti	MPPI-Generic	256	0.2265±0.0433	Intel 13900K	1050 Ti	MPPI-Generic	256	0.2257 ± 0.0578
AMD 5600X	1050 Ti	autorally	256	0.4649±0.0338	Intel 13900K	1050 Ti	autorally	256	0.4543 ± 0.0833
AMD 5600X	1050 Ti	torchrl	256	52.88±2.40	Intel 13900K	1050 Ti	torchrl	256	29.31 ± 2.44
AMD 5600X	1050 Ti	MPPI-Generic	512	0.3077±0.0525	Intel 13900K	1050 Ti	MPPI-Generic	512	0.3016 ± 0.0658
AMD 5600X	1050 Ti	autorally	512	0.4812±0.0375	Intel 13900K	1050 Ti	autorally	512	0.4688 ± 0.0802
AMD 5600X	1050 Ti	torchrl	512	52.97±2.37	Intel 13900K	1050 Ti	torchrl	512	29.91 ± 2.80
AMD 5600X	1050 Ti	MPPI-Generic	1024	0.4373±0.0548	Intel 13900K	1050 Ti	MPPI-Generic	1024	0.4294 ± 0.0753
AMD 5600X	1050 Ti	autorally	1024	0.5196±0.0397	Intel 13900K	1050 Ti	autorally	1024	0.5120 ± 0.0963
AMD 5600X	1050 Ti	torchrl	1024	53.15±2.14	Intel 13900K	1050 Ti	torchrl	1024	29.90 ± 3.00
AMD 5600X	1050 Ti	autorally	2048	0.6371±0.0433	Intel 13900K	1050 Ti	autorally	2048	0.630 ± 0.104
AMD 5600X	1050 Ti	MPPI-Generic	2048	0.8443±0.0614	Intel 13900K	1050 Ti	MPPI-Generic	2048	0.8370 ± 0.0993
AMD 5600X	1050 Ti	torchrl	2048	53.58±2.45	Intel 13900K	1050 Ti	torchrl	2048	30.39 ± 2.92
AMD 5600X	1050 Ti	autorally	4096	1.2952±0.0569	Intel 13900K	1050 Ti	autorally	4096	1.202 ± 0.132
AMD 5600X	1050 Ti	MPPI-Generic	4096	1.4836±0.0616	Intel 13900K	1050 Ti	MPPI-Generic	4096	1.468 ± 0.134
AMD 5600X	1050 Ti	torchrl	4096	55.10±2.42	Intel 13900K	1050 Ti	torchrl	4096	31.28 ± 2.71
AMD 5600X	1050 Ti	autorally	6144	1.4595±0.0618	Intel 13900K	1050 Ti	autorally	6144	1.776 ± 0.151
AMD 5600X	1050 Ti	MPPI-Generic	6144	2.1196±0.0727	Intel 13900K	1050 Ti	MPPI-Generic	6144	2.103 ± 0.155
AMD 5600X	1050 Ti	torchrl	6144	57.43±2.14	Intel 13900K	1050 Ti	torchrl	6144	34.26 ± 2.75
AMD 5600X	1050 Ti	autorally	8192	2.0762±0.0739	Intel 13900K	1050 Ti	autorally	8192	2.360 ± 0.170
AMD 5600X	1050 Ti	MPPI-Generic	8192	2.9062±0.0841	Intel 13900K	1050 Ti	MPPI-Generic	8192	2.893 ± 0.248
AMD 5600X	1050 Ti	torchrl	8192	60.50±2.45	Intel 13900K	1050 Ti	torchrl	8192	37.08 ± 2.68
AMD 5600X	1050 Ti	autorally	16384	4.108±0.113	Intel 13900K	1050 Ti	autorally	16384	4.611 ± 0.255
AMD 5600X	1050 Ti	MPPI-Generic	16384	5.665±0.126	Intel 13900K	1050 Ti	MPPI-Generic	16384	5.638 ± 0.418
AMD 5600X	1050 Ti	torchrl	16384	73.40±1.93	Intel 13900K	1050 Ti	torchrl	16384	51.97 ± 2.88
AMD 5600X	1650	MPPI-Generic	128	0.1459±0.0208	Intel 13900K	1650	MPPI-Generic	128	0.1354 ± 0.0263
AMD 5600X	1650	autorally	128	0.2555±0.0176	Intel 13900K	1650	autorally	128	0.245 ± 0.111
AMD 5600X	1650	torchrl	128	46.52±1.96	Intel 13900K	1650	torchrl	128	24.70 ± 1.77
AMD 5600X	1650	MPPI-Generic	256	0.1530±0.0188	Intel 13900K	1650	MPPI-Generic	256	0.1526 ± 0.0260
AMD 5600X	1650	autorally	256	0.2564±0.0232	Intel 13900K	1650	autorally	256	0.2385 ± 0.0284
AMD 5600X	1650	torchrl	256	52.69±2.31	Intel 13900K	1650	torchrl	256	28.54 ± 1.52
AMD 5600X	1650	MPPI-Generic	512	0.2015±0.0218	Intel 13900K	1650	MPPI-Generic	512	0.1964 ± 0.0320
AMD 5600X	1650	autorally	512	0.2649±0.0226	Intel 13900K	1650	autorally	512	0.2387 ± 0.0249
AMD 5600X	1650	torchrl	512	52.20±2.12	Intel 13900K	1650	torchrl	512	28.67 ± 1.66
AMD 5600X	1650	MPPI-Generic	1024	0.2848±0.0293	Intel 13900K	1650	MPPI-Generic	1024	0.2866 ± 0.0346
AMD 5600X	1650	autorally	1024	0.3260±0.0225	Intel 13900K	1650	autorally	1024	0.3060 ± 0.0306
AMD 5600X	1650	torchrl	1024	52.33±1.78	Intel 13900K	1650	torchrl	1024	28.78 ± 1.65
AMD 5600X	1650	autorally	2048	0.4247±0.0251	Intel 13900K	1650	autorally	2048	0.4047 ± 0.0381
AMD 5600X	1650	MPPI-Generic	2048	0.5046±0.0295	Intel 13900K	1650	MPPI-Generic	2048	0.4834 ± 0.0431
AMD 5600X	1650	torchrl	2048	52.58±2.11	Intel 13900K	1650	torchrl	2048	29.13 ± 1.46
AMD 5600X	1650	autorally	4096	0.8065±0.0447	Intel 13900K	1650	autorally	4096	0.7927 ± 0.0619
AMD 5600X	1650	MPPI-Generic	4096	1.0046±0.0448	Intel 13900K	1650	MPPI-Generic	4096	0.9680 ± 0.0636
AMD 5600X	1650	torchrl	4096	53.69±2.08	Intel 13900K	1650	torchrl	4096	30.61 ± 1.70
AMD 5600X	1650	autorally	6144	0.9841±0.0401	Intel 13900K	1650	autorally	6144	0.9418 ± 0.0623
AMD 5600X	1650	MPPI-Generic	6144	1.2299±0.0437	Intel 13900K	1650	MPPI-Generic	6144	1.1777 ± 0.0637
AMD 5600X	1650	torchrl	6144	55.53±1.80	Intel 13900K	1650	torchrl	6144	32.39 ± 1.72
AMD 5600X	1650	autorally	8192	1.3870±0.0476	Intel 13900K	1650	autorally	8192	1.3343 ± 0.0721
AMD 5600X	1650	MPPI-Generic	8192	1.7740±0.0515	Intel 13900K	1650	MPPI-Generic	8192	1.6789 ± 0.0758
AMD 5600X	1650	torchrl	8192	57.84±2.05	Intel 13900K	1650	torchrl	8192	34.52 ± 1.46
AMD 5600X	1650	autorally	16384	2.7039±0.0685	Intel 13900K	1650	autorally	16384	2.5903 ± 0.0999
AMD 5600X	1650	MPPI-Generic	16384	3.293±0.111	Intel 13900K	1650	MPPI-Generic	16384	3.128 ± 0.128
AMD 5600X	1650	torchrl	16384	68.92±1.73	Intel 13900K	1650	torchrl	16384	46.42 ± 1.73